Domain boundaries in convection patterns

Boris A. Malomed
P. P. Shirshov Institute for Oceanology, 23 Krasikov Street, Moscow, 117218, U.S.S.R.

Alexander A. Nepomnyashchy*
Institute for Continuous Media Mechanics, 1 Academician Korolev Street, Perm', 614013, U.S.S.R.

Michael I. Tribelsky
Organic Intermediates and Dyes Institute "NIOPIK," 1-4 B. Sadovaya Street, Moscow, 103787, U.S.S.R.
(Received 20 March 1990)

Domain boundaries (DB's) in convection patterns are studied near the onset of convection within the framework of amplitude equations of the Newell-Whitehead-Segel type. It is demonstrated that DB's of an arbitrary direction are possible between domains occupied by convection rolls with different orientations. Those DB's are always immobile, and they perform perfect selection of the rolls' wave numbers. In certain particular cases, exact solutions for DB's of this type are found, and their stability against long-wave flexural perturbations is established. DB's between the rolls and a hexagonal pattern in the slightly overcritical case, and between the hexagons and the conduction (quiescent) state in the slightly subcritical case, are investigated as well. In this case, the DB is, generally speaking, moving with a constant velocity. The exponentially weak effect of pinning of the moving DB by a small-scale underlying structure is studied. Formation of DB's of the "quiescent-state–hexagon" and "roll-hexagon" types near a sidewall is also investigated. The special case of a DB between two systems of rolls, the angle between which is close to $\pi/3$ or $2\pi/3$, is studied in detail. This DB is, as a matter of fact, a bound state of two DB's of the "roll-hexagon" type. Finally, it is demonstrated that in one-dimensional patterns (rolls) a stationary DB is not possible. In this case, a dynamical problem of decay of a DB-like structure is solved.

I. INTRODUCTION

The onset of Rayleigh-Benard convection in a layer of liquid heated from below is a typical example of formation of a nonlinear dissipative structure in nonequilibrium systems. According to linear stability theory (see, e.g., the book by Gershuni and Zhukhovitsky[1]), perturbations with horizontal wave vectors $\mathbf{k}$ of an arbitrary orientation, the modulus of which lies in a narrow region near a critical value k_c, start increasing when the Rayleigh number R exceeds a critical value R_c. Nonlinear patterns resulting from the instability are rather various. The most well-studied patterns are convection rolls.[2] In an experiment, the rolls are usually initiated by imposing a spatially periodic perturbation upon the unstable conduction state.[3–5] However, the patterns which develop from random perturbations are, as a rule, irregular and contain various defects: dislocations, domain boundaries (which are also frequently called grain boundaries), roll distortion, etc.[3–5] Alongside the random initial perturbations, defects may be induced by a regular influence of lateral walls. The study of dynamics of solitary defects is a necessary step of investigation of spatiotemporal complexity of convection patterns.

The type of defect which is, so far, most well studied both theoretically and experimentally is a dislocation in a system of the parallel rolls (see, e.g., Refs. 6–10). Another type of defect, which is studied in much less detail, is a linear defect in the form of a domain boundary (DB) sandwiched between regions (domains) filled by different regular patterns, including DB between rolls of different orientations.[11–14]

In this paper we develop a systematic analysis of the DB's near the onset of convection, i.e., in a slightly overcritical or slightly subcritical situation. The analysis is based on amplitude equations, such as the Newell-Whitehead-Segel equation,[15,16] and coupled Ginzburg-Landau equations.[14] These equations are introduced in Sec. II. Section III is devoted to DB's between domains occupied by rolls with different orientations of their wave vectors, orientation of the linear DB relative to those wave vectors being arbitrary. A solution looked for is a linear superposition of the two systems of rolls with slowly varying amplitudes. The evolution of the amplitudes is governed by a system of coupled Ginzburg-Landau (GL) equations. It is demonstrated that this DB is always immobile, and it uniquely selects wave numbers (i.e., moduli of the wave vectors) of the rolls. In certain particular cases, exact solutions of the above-mentioned coupled GL equations that describe the DB are found. In those cases it is proved that the DB is stable against long-wave flexural perturbations of its "crest." In a general case, we find the form of the DB numerically. At the end of Sec. III, we study the DB of the "roll-roll" type in the case

when the "refraction angle" of the rolls at the DB is small. In this case, the whole pattern is approximated not by a linear superposition of two systems of rolls, but by a single family of rolls with a slowly varying amplitude governed by the Newell-Whitehead-Segel (NWS) equation. We demonstrate that in this situation the NWS equation reduces to the Cahn-Hilliard (CH) equation for a local wave number, and the DB corresponds to the well-known kink solution of the CH equation. This DB can be proved to be stable. We also demonstrate that a stationary DB cannot exist between domains with parallel wave vectors (i.e., with the zero refraction angle) and different wave numbers. We investigate decay of an initial configuration of a DB-like form. The decay is governed by a nonlinear diffusion equation for a local wave number.

In Sec. IV we consider various types of DB's involving the hexagonal pattern. This pattern may be regarded as a superposition of three systems of rolls whose wave vectors form a closed triangle. As is known,[17,18] the hexagons are stable sufficiently close to the onset (both in the subcritical and supercritical ranges) if weak non-Boussinesq effects, which break the symmetry of the problem relative to the middle plane of the convective layer, are taken into account (temperature dependence of viscosity, thermocapillary effect, deformation of the free upper boundary of the layer, and so on). These effects give rise to small resonant (quadratic) additional couplings in a system of three coupled Ginzburg-Landau equations governing amplitudes of the hexagonal pattern.[14] As is well known,[17,18] the hexagons coexist with the stable conduction (quiescent) state in the subcritical range, and with the rolls in the overcritical range. In accordance with this, we study the DB's between the hexagons and the conduction state, and between the hexagons and the rolls. The DB solution can be obtained analytically in one particular case; in the general case we find it numerically. Unlike the DB's of the roll-roll type, the ones separating the hexagons and a pattern of another type move with a constant velocity proportional to the difference of the Lyapunov functional densities of the two patterns separated by the DB. We find numerically a dependence of the velocity on an angle determining the orientation of the DB relative to the hexagons. We reveal that this dependence, i.e., an effective anisotropy of the system, is very weak. We also consider the exponentially weak effect of pinning of the DB by the underlying small-scale structure. This effect is nonadiabatic, i.e., it cannot be comprised by the amplitude equation. The pinning takes place provided the DB is nearly perpendicular to any wave vector of the pattern. In the same section, we consider the DB of the roll-roll type in the special case when the angle between wave vectors of the two systems of rolls is $\pi/3$ or $2\pi/3$. In this case, the resonant interaction generates a layer of the hexagons sandwiched between the rolls, so that the corresponding DB is, as a matter of fact, a bound state of two DB's of the "roll-hexagon" type. At the end of Sec. IV, we analyze formation of the DB's of the "roll-hexagon" and "hexagon–quiescent-state" types near a sidewall. We demonstrate that in the case when the hexagons quench, respectively, the rolls or the quiescent state, the DB is necessary to match the hexagonal pattern in the bulk of the system to the rolls or the quiescent state selected by the sidewall.

As is known, in some "exotic" cases (e.g., convection between nearly heat-insulating boundaries[19,20]) the basic stable patterns are square (or, more generally, rectangular[21]) cells instead of the rolls. The square patterns with different orientations may also form a DB. This problem is briefly considered in Sec. V.

At last, in concluding Sec. VI we discuss possibilities of experimental observation of the DB's studied in this work. A short account of the results obtained in the present work has been given previously in Ref. 22.

To conclude the Introduction, it is pertinent to note that linear defects of the DB type (grain boundaries) are well known in liquid-crystal convection; see, e.g., the corresponding experimental observations in Ref. 23 and theoretical analysis in Ref. 24. The amplitude equations governing convection patterns in liquid crystals have, generally speaking, a form differing from that for isotropic liquids. Analysis of the DB's in liquid-crystal convection patterns lies beyond the framework of the present work.

II. AMPLITUDE EQUATIONS

The state of a horizontal convective layer is described by the set of variables $U=(\mathbf{v},T,p)$, where $\mathbf{v}$, T, and p stand, respectively, for the velocity, departure of temperature from the heat-conductivity profile, and departure of pressure from the hydrostatic profile. We assume that the Rayleigh number R is close to the critical value R_c, i.e.,

$$\epsilon \equiv (R-R_c)/R_c \tag{2.1}$$

is a small parameter. Note that we will deal both with positive and with negative ϵ. These cases are referred to as slightly overcritical and slightly subcritical ones, respectively. As is known,[1] at $R=R_c$ the convective instability to perturbations with wave vectors lying in a horizontal plane sets in at a finite wave number k_c of a perturbation. In what follows, we measure the wave numbers in units of k_c, i.e., we set $k_c=1$. At small ϵ [see Eq. (2.1)] and small departure of the instability wave number k from $k_c\equiv 1$, a dimensionless instability growth rate $\sigma(\epsilon,k)$ may be expanded as follows:

$$\sigma=\epsilon-(k^2-1)^2+O((k^2-1)^3,\epsilon(k^2-1)) . \tag{2.2}$$

According to Eq. (2.2), at $\epsilon>0$ the growing perturbations have wave numbers lying in the interval

$$|k^2-1|\le\sqrt{\epsilon}+O(\epsilon) , \tag{2.3}$$

while orientation of their wave vectors in the horizontal plane is arbitrary.

To derive an amplitude equation governing slow evolution of a near-onset convection pattern, one should represent the convective flow in the form

$$U(\mathbf{r},z,t)=\sum_{l=1}^{N}[u_l(z)a_l(x_l,y_l,t)e^{ik_c x_l}+\text{c.c.}]+O(\epsilon)\ , \tag{2.4}$$

where t is time, $\mathbf{r}$ is the horizontal radius vector, z is the vertical coordinate, $u_l(z)$ are the so-called modal functions, $x_l \equiv \mathbf{r}\cdot\mathbf{n}_l$, $y_l \equiv \mathbf{r}\cdot\boldsymbol{\tau}_l$, $\mathbf{n}_l$ and $\boldsymbol{\tau}_l$ are pairs of mutually orthogonal unit vectors lying in the horizontal plane, and $a_l = O(\sqrt{\epsilon})$ are slowly varying amplitudes of N independent modes, the superposition of which gives a convection pattern according to Eq. (2.4). The amplitudes are governed by the closed systems of coupled Newell-Whitehead-Segel equations

$$\frac{\partial a_l}{\partial t}=\left\{\left[\epsilon+4\left[\frac{\partial}{\partial x_l}-\frac{i}{2}\frac{\partial^2}{\partial y_l^2}\right]^2\right]-\sum_{j=1}^{N}\kappa_{lj}|a_j|^2\right\}a_l+\alpha a_m^* a_n^*,\quad l=1,2,\ldots,N \tag{2.5}$$

where κ_{lj} are the so-called matrix elements of the nonlinear intermode interaction, the indices m and n are such that $\mathbf{n}_l+\mathbf{n}_m+\mathbf{n}_n=\mathbf{0}$, i.e., the modes with the numbers l, m, and n constitute a resonantly coupled triad, and α is the matrix element of the resonant interaction. The coefficients κ_{lj} depend only on the angle θ_{lj} between the unit vectors $\mathbf{n}_l$ and $\mathbf{n}_j$, and also on boundary conditions adopted in the convection problem. The coefficient $\kappa(\theta)$ has been first calculated for a layer with solid isothermal boundaries by Schlüter, Lortz, and Busse in Ref. 25. Note that the positiveness of $\kappa_{ll}\equiv\kappa(\theta=0)$ was ascertained as early as in 1954 by means of a variational principle.[26] As was mentioned above, the quadratic term in Eq. (2.5) takes account of weak effects violating the symmetry with respect to the transformation $z\to -z$, so that the coefficient α is typically small.[17,18]

An important property of the system of coupled equations (2.5) (which is not shared by the underlying hydrodynamic equations of the convection theory) is the presence of the Lyapunov functional F:

$$\frac{\partial a_l}{\partial t}=-\frac{\delta F}{\delta a_l^*}\ , \tag{2.6a}$$

$$F\equiv\int d\mathbf{r}\left\{\sum_l\left[-\epsilon|a_l|^2+4\left|\left[\frac{\partial}{\partial x_l}-\frac{i}{2}\frac{\partial^2}{\partial y_l^2}\right]^2 a_l\right|^2\right]+\tfrac{1}{2}\sum_{l,j}\kappa_{lj}|a_l|^2|a_j|^2+\tfrac{1}{3}\alpha\sum_{l,m,n}(a_l a_m a_n+a_l^* a_m^* a_n^*)\right\}\ . \tag{2.6b}$$

It is assumed that the summation in the last term on the right-hand side comprises the resonance triads only. Equation (2.6a) entails the inequality

$$\frac{dF}{dt}=-2\int d\mathbf{r}\left|\frac{\delta F}{\delta a}\right|^2\le 0\ , \tag{2.7}$$

hence at $t\to\infty$ the system must approach a stationary state which provides a minimum of the functional F.

Stationary spatially periodic or quasiperiodic convection patterns corresponds to solutions of Eq. (2.5) of the form

$$a_l=r_l e^{iq_l x_l},\quad r_l\sim\sqrt{\epsilon},\quad q_l^2\lesssim\epsilon\ , \tag{2.8}$$

with constant r_l and q_l ($l=1,\ldots,N$). In particular, $N=1$, 2, and 3 give rise to rolls, rectangles, and hexagons, respectively (in the last case, the three modes must constitute a resonance triad). In the case $\alpha=0$, $\kappa(\theta)\ge\kappa(0)$ at $\theta>0$, the only stable patterns are rolls, the wave-number detuning q_1 of which from $q_1=1$ lies inside a certain interval.[25,15] If $\kappa(\theta)\ge\kappa(0)$ but $\alpha\neq 0$, the stable rolls may coexist with stable hexagons. In the case when there are values of θ such that $\kappa(\theta)<\kappa(0)$, the rolls are unstable, and the fundamental types of the stable patterns are rectangles with angles θ between the unit wave vectors $(\mathbf{n}_1,\mathbf{n}_2)$ for which $\kappa(\theta)<\kappa(0)$.[19,21] If $\alpha\neq 0$, the rectangles may coexist with the hexagons.[21] The stability intervals of the wave-number detunings [in the cases $q_1=q_2\neq 1$ and $q_1=1$, $q_2\neq q_1$ for the rectangles; $q_1=q_2=q_3$ for the hexagons] have been found in Ref. 21. In the case of coexistence of the rolls with the hexagons, their stability against finite perturbations was investigated in Ref. 27.

At last, the case $N\ge 4$ in Eq. (2.8) gives rise to quasiperiodic patterns with the symmetry of a two-dimensional quasicrystal. These patterns and their stability have been studied in detail in Refs. 28.

The multistability may give rise to a situation when different dynamical regimes are established in different parts of the convective layer, provided its aspect ratio is sufficiently large. This possibility broaches the problem of boundaries separating different patterns. These may be patterns of the same type differing in wave vectors (DB's roll-roll, hexagon-hexagon, or rectangle-rectangle), or patterns of different types (roll-hexagon, hexagon–quiescent state, or rectangle-hexagon). Let us emphasize that in this work we confine ourselves to boun-

daries between locally stable patterns, and we do not touch the problem of propagation of a front of transition from an unstable state into a stable one (see, e.g., Refs. 29 and 30).

III. ROLL-ROLL DOMAIN BOUNDARIES

A. Formulation of the problem

In this section we will deal with the case $\alpha=0$ [see Eq. (2.5)], when the only stable uniform patterns are the rolls. A superposition of the rolls with wave vectors $\mathbf{k}_1$ and $\mathbf{k}_2$ is described by the system of two coupled NWS equations (2.5):

$$\frac{\partial a_1}{\partial t}=\left[\epsilon+4\left[\frac{\partial}{\partial x_1}-\frac{i}{2}\frac{\partial^2}{\partial y_1^2}\right]^2\right]a_1-\kappa(0)|a_1|^2a_1 -\kappa(\theta_1-\theta_2)|a_2|^2a_1 , \tag{3.1a}$$

$$\frac{\partial a_2}{\partial t}=\left[\epsilon+4\left[\frac{\partial}{\partial x_2}-\frac{i}{2}\frac{\partial^2}{\partial y_2^2}\right]^2\right]a_2-\kappa(0)|a_2|^2a_2 -\kappa(\theta_1-\theta_2)|a_1|^2a_2 , \tag{3.1b}$$

where $\theta_{1,2}$ are the angles between the vectors $\mathbf{k}_{1,2}$ and the x axis [Fig. 1(a)]. The DB solution is singled out by the boundary conditions

$$\frac{\nabla a_1}{a_1}=i(k_1-1)\mathbf{n}_1,\quad a_2=0 \text{ at } x=-\infty , \tag{3.2a}$$

$$\frac{\nabla a_2}{a_2}=i(k_2-1)\mathbf{n}_2,\quad a_1=0 \text{ at } x=+\infty , \tag{3.2b}$$

where $k_{1,2}\equiv|\mathbf{k}_{1,2}|$, $\mathbf{n}_{1,2}\equiv\mathbf{k}_{1,2}/k_{1,2}$. The partial derivatives in Eqs. (3.1) are expressed in terms of $\partial/\partial x$ and $\partial/\partial y$ as follows:

$$\frac{\partial}{\partial x_l}\equiv\cos\theta_l\frac{\partial}{\partial x}+\sin\theta_l\frac{\partial}{\partial y} ,$$

$$\frac{\partial}{\partial y_l}\equiv-\sin\theta_l\frac{\partial}{\partial x}+\cos\theta_l\frac{\partial}{\partial y} .$$

Let us look for a solution corresponding to a plane DB perpendicular to the x axis:

$$a_l=\left[\frac{\epsilon}{\kappa(0)}\right]^{1/2}B_l(x)e^{i(k_l-1)(\sin\theta_l)y} . \tag{3.3a}$$

We assume that neither angle θ_l is close to $\pi/2$ (the case when $\mathbf{k}_1$ is parallel to the DB, and $\mathbf{k}_2$ is perpendicular to it, was analyzed earlier in Refs. 12 and 13). The scale transformation

$$T\equiv|\epsilon|t,\quad X=\tfrac{1}{2}\sqrt{|\epsilon|}x \tag{3.3b}$$

[we write $|\epsilon|$ instead of ϵ with intention to employ the rescaled variables (3.3) in the subcritical case $0<-\epsilon\ll1$ too] brings Eqs. (3.1) and (3.2) into the following form (where corrections of higher orders in ϵ have been omitted):

$$\frac{\partial B_1}{\partial T}=\left[\cos\theta_1\frac{\partial}{\partial X}+i(\sin^2\theta_1)q_1\right]^2B_1+B_1-|B_1|^2B_1 -g|B_2|^2B_1 , \tag{3.4a}$$

$$\frac{\partial B_2}{\partial T}=\left[\cos\theta_2\frac{\partial}{\partial X}+i(\sin^2\theta_2)q_2\right]^2B_2+B_2-|B_2|^2B_2 -g|B_1|^2B_2 , \tag{3.4b}$$

$$\frac{1}{B_1}\frac{\partial B_1}{\partial X}=iq_1\cos\theta_1,\quad B_2=0 \text{ at } X\to-\infty , \tag{3.5a}$$

$$\frac{1}{B_2}\frac{\partial B_2}{\partial X}=iq_2\cos\theta_2,\quad B_1=0 \text{ at } X\to+\infty , \tag{3.5b}$$

where[31]

$$q_l\equiv2(k_l-1)/\sqrt{\epsilon} ,\qquad g(\theta_1-\theta_2)\equiv\kappa(\theta_1-\theta_2)/\kappa(0) . \tag{3.6}$$

In this paper, except for Sec. V, we assume $g>1$, otherwise the rolls cannot be a locally stable pattern.

The substitution

$$B_l=A_l\exp\left[-i\frac{\sin^2\theta_l}{\cos\theta_l}q_lX\right],\quad l=1,2 \tag{3.7}$$

transforms the boundary problem based on Eqs. (3.4) and

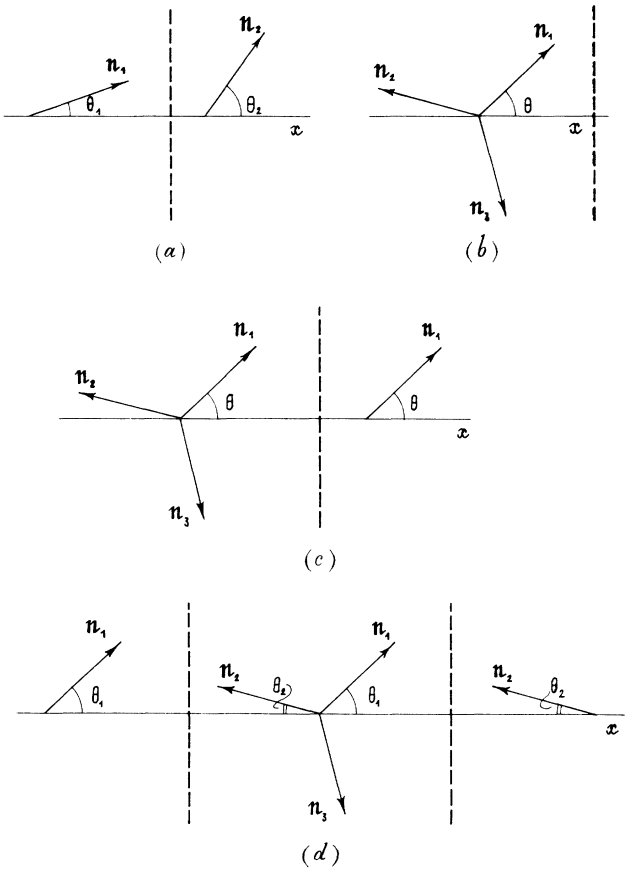

FIG. 1. Different types of domains boundaries. The vertical dashed lines depict the domain boundary itself, and the arrows are the unit vectors $\mathbf{n}_l$ that determine orientation of different modes [see Eq. (2.4)]: (a) roll-roll; (b) hexagon–quiescent state; (c) hexagon-roll; (d) the "resonant" domain boundary roll-hexagon-roll ($\theta_1+\theta_2=\pi/3$ or $\theta_1+\theta_2=2\pi/3$).

(3.5) into the system of coupled Ginzburg-Landau equations:

$$(A_1)_T = D_1(A_1)_{XX} + (1 - |A_1|^2 - g|A_2|^2)A_1 , \quad (3.8a)$$

$$(A_2)_T = D_2(A_2)_{XX} + (1 - |A_2|^2 - g|A_1|^2)A_2 , \quad (3.8b)$$

complemented by the following boundary conditions:

$$(A_1)_X / A_1 = iQ_1, \quad A_2 = 0 \text{ at } X \to -\infty , \quad (3.9a)$$

$$(A_2)_X / A_2 = iQ_2, \quad A_1 = 0 \text{ at } X \to +\infty , \quad (3.9b)$$

where

$$D_l \equiv \cos^2\theta_l, \quad Q_l \equiv q_l / \cos\theta_l \quad (l = 1,2) . \quad (3.10)$$

B. Wave-number selection

First of all, let us find out which conditions are necessary for existence of stationary solutions of the boundary problem based on Eqs. (3.8) and (3.9). Setting

$$A_l = r_l e^{i\varphi_l}, \quad \varphi_l' \equiv K_l \quad (3.11)$$

(with real r_l and φ_l) brings the stationary version of Eqs. (3.8) ($\partial/\partial T = 0$) into the form

$$D_1 r_1'' + r_1(1 - D_1 K_1^2 - r_1^2 - g r_2^2) = 0 , \quad (3.12a)$$

$$D_2 r_2'' + r_2(1 - D_2 K_2^2 - r_2^2 - g r_1^2) = 0 , \quad (3.12b)$$

$$r_l K_l' + 2 r_l' K_l = 0 \quad (l = 1,2) , \quad (3.12c)$$

where the prime stands for d/dX. As it follows from Eqs. (3.12c), the quantities $M_l \equiv r_l^2 K_l$ are constants. On the other hand, r_l vanish at either infinity according to the boundary conditions (3.9). A simple analysis shows that these two conditions (M_l = const and $r_l \to 0$) are compatible only in the case $M_l = 0$. The situation resembles the well-known result of classical mechanics: A particle with nonzero angular momentum cannot reach the center of an axially symmetric potential.

Thus a stationary DB is only possible if $K_1 = K_2 \equiv 0$. According to Eqs. (3.11) and (3.9b), this means $Q_1 = Q_2 = 0$. This result implies that a stationary DB performs perfect wave-number selection: $k = 1$ [see Eqs. (3.11) and (3.6)]. As is well known, the same effect is produced by a heat-insulating side wall[32] or a so-called ramp, i.e., smoothly matching a region with $\epsilon < 0$.[33] In all the cases, the reason for the perfect wave-number selection is essentially the same. The quantity $M_l = r^2 K_l$, which is a constant, vanishes in a certain asymptotic region (at $X \to \pm\infty$ in our case), hence it must be zero everywhere, i.e., $K_l \equiv 0$.

To investigate dynamics of the wave-number selection, we have performed numerical integration of the evolution equations (3.8) with initial data satisfying the boundary conditions (3.9). As is shown in Fig. 2, the values of $|K_1|$ and $|K_2|$ monotonically decrease in the region where the DB is formed. At large times, the size of the region adjacent to the DB, where the initial values of $|K_{1,2}|$ have been strongly damped, grows $\sim\sqrt{t}$ (cf. the analysis of the decay of a DB-like configuration in the one-dimensional geometry performed below in Sec. III E).

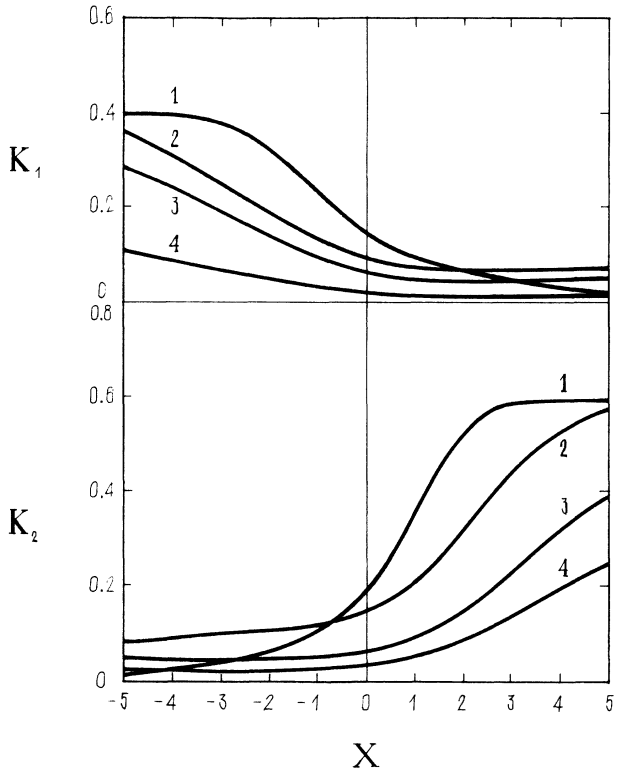

FIG. 2. Dynamics of the wave-number selection process. A typical example of evolution of the profiles of the wave-number detunings K_1 and K_2: (1) $T = 1$; (2) $T = 5$; (3) $T = 20$; (4) $T = 50$.

It can be demonstrated that, if higher terms, such as A_{XXX}, $|A|^2 A_X$, and $A^2 A_X^*$, are added to the amplitude equations (3.8), the selected wave number k_* remains uniquely determined with the only difference that $k_* = 1 + O(\epsilon)$.

So, we have obtained the necessary condition for the existence of DB: $Q_1 = Q_2 = 0$. Let us now prove that a DB solution exists indeed. In the case $Q_1 = Q_2 = 0$, the stationary versions ($\partial/\partial T = 0$) of Eqs. (3.8) take the form

$$D_1 r_1'' + r_1(1 - r_1^2 - g r_2^2) = 0 , \quad (3.13a)$$

$$D_2 r_2'' + r_2(1 - r_2^2 - g r_1^2) = 0 . \quad (3.13b)$$

The boundary conditions to Eqs. (3.13) are

$$r_1 = 1, \quad r_2 = 0 \text{ at } X \to -\infty , \quad (3.14a)$$

$$r_1 = 0, \quad r_2 = 1 \text{ at } X \to +\infty . \quad (3.14b)$$

Equations (3.13) describe motion of a mechanical particle with the Lagrangian

$$L = \tfrac{1}{2} D_1 (r_1')^2 + \tfrac{1}{2} D_2 (r_2')^2 - U , \quad (3.15)$$

$$U = \tfrac{1}{2}(r_1^2 + r_2^2) - \tfrac{1}{4}(r_1^4 + 2 g r_1^2 r_2^2 + r_2^4) . \quad (3.16)$$

It is straightforward to see that the Lagrangian (3.15) coincides with the density of the Lyapunov functional defined by Eq. (2.6b). The roll patterns (3.14a) and (3.14b) provide maxima of the effective potential (3.16),

i.e., minima of the Lyapunov functional (2.6b) [Lagrangian (3.15)]. A DB solution corresponds to a separatrix trajectory connecting the two potential maxima. A simple qualitative analysis of the mechanical problem demonstrates that there always exists at least one separatrix trajectory of this type.

C. Analytical solutions

In a general case, the boundary problem given by Eqs. (3.13) and (3.14) admits only a numerical solution. A typical example of this solution is shown in Fig. 3. Let us emphasize that in the "oblique" case ($\theta_1 \neq -\theta_2$, as in the example shown in Fig. 3) the DB of the roll-roll type exists as well as in the symmetric configuration ($\theta_1 = -\theta_2$) which seems more "natural."

The DB solution can be found analytically in certain particular cases. We first dwell on the case

$$0 < g - 1 \ll 1 \tag{3.17}$$

(recall that the rolls lose the local stability at $g < 1$, when rectangles become a stable pattern). In this case, the effective potential (3.16) is nearly axisymmetric. Following the lines of Ref. 11, we introduce the polar variables

$$r_1 = r\cos\chi, \quad r_2 = r\sin\chi \ . \tag{3.18}$$

It is easy to see that r and χ are functions of the slow coordinate

$$\xi \equiv (g-1)^{1/2} X \ , \tag{3.19a}$$

and the function $r(\xi)$ is almost constant:

$$r(\xi) = 1 + (g-1)R(\xi), \quad R(\xi) = O(1) \ . \tag{3.19b}$$

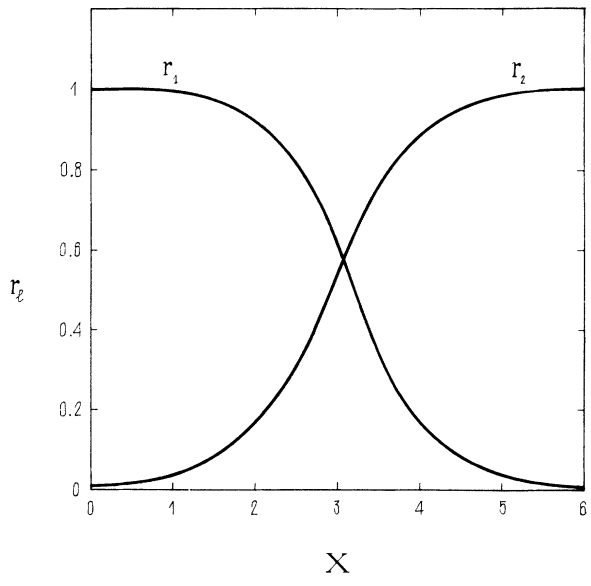

FIG. 3. The domain-boundary solution of Eqs. (3.13), (3.14) in the case $D_1 = \frac{1}{4}$, $D_2 = \frac{1}{2}$, $g \equiv 2$ [this corresponds to the well-known Swift-Hohenberg model (Ref. 43), in which $g(\theta)$ does not depend on θ, i.e., $g(\theta) \equiv 2$].

According to Eq. (3.19), Eqs. (3.13) in the lowest approximation reduce to the single equation for the phase variable $\chi(\xi)$:

$$\tfrac{1}{2} D(\chi) \left[\frac{d\chi}{d\xi} \right]^2 - \tfrac{1}{8}\sin^2(2\chi) = 0 \ , \tag{3.20}$$

where $D(\chi) \equiv (\cos^2\theta_1)(\sin^2\chi) + (\cos^2\theta_2)(\cos^2\chi)$, and the boundary conditions (3.14) take the form

$$\chi(\xi \to -\infty) \to 0, \quad \chi(\xi \to +\infty) \to \pi/2 \ . \tag{3.21}$$

The boundary problem (3.20),(3.21) admits the analytical solution

$$\xi - \xi_0 = \frac{1}{2} \left[(\cos\theta_1) \ln \left| \frac{\sqrt{D(\chi)} + \cos\theta_1}{\sqrt{D(\chi)} - \cos\theta_1} \right| + (\cos\theta_2) \ln \left| \frac{\sqrt{D(\chi)} - \cos\theta_2}{\sqrt{D(\chi)} + \cos\theta_2} \right| \right] . \tag{3.22}$$

In the symmetric case $\theta_1 = -\theta_2 \equiv \theta$ (this case was considered by Cross[11]), the function $\chi(\xi)$ defined implicitly by Eq. (3.22) is reduced to the well-known sine-Gordon kink:

$$\chi = \tan^{-1}\exp[(\xi - \xi_0)/\cos\theta] \ . \tag{3.23}$$

The linear density of the Lyapunov functional (3.15) for the DB (its "surface energy"), determined by Eqs. (3.18) and (3.19), is given, in terms of Eqs. (3.18) and (3.19), by the following expression:

$$\mathcal{F} \equiv \int_{-\infty}^{+\infty} dX [L(X) - L(\infty)] = (g-1)^{1/2} \int_{-\infty}^{+\infty} d\xi \left[\tfrac{1}{2} D(\chi) \left[\frac{d\chi}{d\xi} \right]^2 + \tfrac{1}{8}\sin^2(2\chi) \right] . \tag{3.24}$$

Insertion of Eq. (3.22) into Eq. (3.24) yields

$$\mathcal{F} = \tfrac{1}{3}[g(\theta_1 - \theta_2) - 1]^{1/2} (\cos^2\theta_1 + \cos\theta_1\cos\theta_2 + \cos^2\theta_2) \times (\cos\theta_1 + \cos\theta_2)^{-1} \ . \tag{3.25}$$

According to the definition adopted in Fig. 1(a), it is assumed here that $|\theta_{1,2}| < \pi/2$, $\theta_1 \neq \theta_2$.

Another exact solution can be obtained in the case $\theta_1 = -\theta_2 \equiv \theta$, $g = 3$:

$$r_1 = \frac{1}{2} \left[1 - \tanh \left[\frac{X}{\sqrt{2}\cos\theta} \right] \right] , \tag{3.26a}$$

$$r_2 = \frac{1}{2} \left[1 + \tanh \left[\frac{X}{\sqrt{2}\cos\theta} \right] \right] . \tag{3.26b}$$

In this case, the Lyapunov functional density is

$$\mathcal{F} = (\sqrt{2}/3)\cos\theta \ . \tag{3.27}$$

In conclusion, let us note that, due to scaling properties of the underlying boundary-value problem based on Eqs. (3.13) and (3.14), in a general case the functional density can be represented in the form

$$\mathcal{F}(\theta_1,\theta_2)=f(g(\theta_1-\theta_2),\cos\theta_2/\cos\theta_1)\cos\theta_1 . \quad (3.28)$$

Here $f(g,x)$ is a function possessing the property $f(g,x)=f(g,1/x)x$ induced by the symmetry of the underlying problem with respect to the replacement $\theta_1 \rightleftarrows \theta_2$. For the symmetric DB ($\theta_1=-\theta_2\equiv\theta$) $\mathcal{F}=f(g(2\theta),1)\cos\theta$.

D. Stability of the domain boundary

1. One-dimensional perturbations

To proceed to the investigation of stability of the roll-roll DB, we first dwell on one-dimensional perturbations independent of the y coordinate. Taking a perturbed solution to Eqs. (3.8) in the form

$$A_l=[r_l(X)+\tilde{r}_l(X,T)]\exp[i\tilde{\varphi}(X,T)] \quad (3.29)$$

($l=1,2$), and linearizing the equations in $\tilde{r}_l$ and $\tilde{\varphi}_l$, one arrives at the following eigenvalue problem for the instability growth rate σ ($r_l,\tilde{\varphi}_l\sim e^{\sigma t}$):

$$\sigma\tilde{r}_1=D_1\tilde{r}_1''+(1-3r_1^2-gr_2^2)\tilde{r}_1-2gr_1r_2\tilde{r}_2 , \quad (3.30a)$$

$$\sigma\tilde{r}_2=D_2\tilde{r}_2''+(1-3r_2^2-gr_1^2)\tilde{r}_2-2gr_2r_1\tilde{r}_1 , \quad (3.30b)$$

$$\sigma r_1\tilde{\varphi}_1=D_1(r_1\tilde{\varphi}_1''+2r_1'\tilde{\varphi}_1') , \quad (3.31a)$$

$$\sigma r_2\tilde{\varphi}_2=D_2(r_2\tilde{\varphi}_2''+2r_2'\tilde{\varphi}_2'') , \quad (3.31b)$$

where the prime again stands for d/dX. As we see, the equations for the amplitude and phase perturbations decouple. Stability of a DB which provides a minimum of the Lyapunov functional (3.15) against the amplitude perturbations is provided by the inequality (2.6a), i.e., by the existence of the Lyapunov functional. However, it is known that, generally speaking, this fact does not guarantee the stability against *phase* perturbations: It is possible that a boundary problem endowed with the Lyapunov functional has no stable stationary solution at all. The well-known example is the one-dimensional GL equation,

$$A_t=A_{xx}+A(1-|A|^2) ,$$

with the boundary condition $A(x\to+\infty)=-A(x\to-\infty)=1$. The only stationary solution to this boundary problem is the kink $A=\tanh(x/\sqrt{2})$, which is, however, unstable against phase perturbations. Therefore, below we perform analysis of the stability of the DB solution against phase perturbations.

Multiplying Eqs. (3.31) by $r_l\tilde{\varphi}_l$ and integrating yields

$$\sigma_l=-D_l\int_{-\infty}^{+\infty}r_l^2(\tilde{\varphi}_l')^2dX\Big/\int_{-\infty}^{+\infty}r_l^2\tilde{\varphi}_l^2dX \quad (3.32)$$

($l=1,2$). Evidently, the eigenvalues (3.32) are negative, which guarantees the stability against the phase perturbations.

If the DB is stable against small perturbations, it may be metastable in the sense that its decay into a pair of other DB's lowers the Lyapunov functional density $\mathcal{F}$. In other words, it is necessary to find out whether there exists, for given θ_1 and θ_2, an angle θ_3 for which

$$\mathcal{F}(\theta_1,\theta_3)+\mathcal{F}(\theta_3,\theta_2)<\mathcal{F}(\theta_1,\theta_2) . \quad (3.33)$$

The inequality (3.33) implies that a layer of rolls with a new wave vector with the orientation angle θ_3 intervenes between the rolls with the ones θ_1 and θ_2 (it is implied that the two newly formed DB's are parallel to the original DB).

This question can be answered explicitly in the special case (3.17) admitting the analytical solution for DB's. If, for instance, we deal with the explicitly tractable case (3.17), we conclude, using the explicit formula (3.25) for the Lyapunov functional density, that the *symmetric* DB ($\theta_1=-\theta_2\equiv\theta$) is stable against the decay into a pair of new ones unless

$$16g\left(\frac{\pi}{2}-\theta\right)<9g(2\theta)+7 , \quad (3.34)$$

provided $dg/d\theta\le 0$ [the inequality (3.34) is a corollary of the one (3.33)].

2. Two-dimensional perturbations

The eigenvalue problem for the instability growth rate of two-dimensional perturbations can be obtained from Eqs. (3.30) and (3.31) if one changes $\cos\theta_l d/dX$ (recall $D_l\equiv\cos^2\theta_l$) to

$$\frac{\partial}{\partial X_l}\equiv\cos\theta_l\frac{\partial}{\partial X}+\sin\theta_l\frac{\partial}{\partial Y}$$

[$l=1$ for Eqs. (3.30a) and (3.31a), and $l=2$ for Eqs. (3.30b) and (3.31b)], where $Y\equiv\frac{1}{2}\sqrt{|\epsilon|}y$, cf. Eq. (3.3). For the particular type of the two-dimensional perturbations of the form $f(X)\exp(iqY)$ we obtain the equations

$$\sigma\tilde{r}_1=\left(\cos\theta_1\frac{d}{dX}+iq\sin\theta_1\right)^2\tilde{r}_1+(1-3r_1^2-gr_2^2)\tilde{r}_1 -2gr_1r_2\tilde{r}_2 , \quad (3.35a)$$

$$\sigma\tilde{r}_2=\left(\cos\theta_2\frac{d}{dX}+iq\sin\theta_2\right)^2\tilde{r}_2+(1-3r_2^2-gr_1^2)\tilde{r}_2 -2gr_2r_1\tilde{r}_1 , \quad (3.35b)$$

$$\sigma r_1\tilde{\varphi}_1=r_1\left(\cos\theta_1\frac{d}{dX}+iq\sin\theta_1\right)^2\tilde{\varphi}_1 +2r_1'\cos\theta_1\left(\cos\theta_1\frac{d}{dX}+iq\sin\theta_1\right)\tilde{\varphi}_1 , \quad (3.36a)$$

$$\sigma r_2\tilde{\varphi}_2=r_2\left(\cos\theta_2\frac{d}{dX}+iq\sin\theta_2\right)^2\tilde{\varphi}_2 +2r_2'\cos\theta_2\left(\cos\theta_2\frac{d}{dX}+iq\sin\theta_2\right)\tilde{\varphi}_2 . \quad (3.36b)$$

For the phase perturbations we obtain from Eqs. (3.36), similarly to Eq. (3.32),

$$\sigma_l=-q^2\sin^2\theta_l-\cos^2\theta_l\frac{\int_{-\infty}^{+\infty}r_l^2(\tilde{\varphi}_l')^2dX}{\int_{-\infty}^{\infty}r_l^2\tilde{\varphi}_l^2dX} , \quad (3.36')$$

i.e., the phase perturbations do not give rise to an instability. As for the amplitude perturbations, among them most "dangerous" are the long-wave perturbations, which give rise to a periodic distortion of the DB at a large scale (in the y direction). At $q\to 0$, this mode of perturbations goes over into a shift (Goldstone) mode with the zero instability growth rate. Let us look for the long-wave distortion mode in the form

$$\tilde{r}_l(X)=r_l'(X)+iq\sin(2\theta_l)\tilde{r}_l^{(1)}(X)+\cdots . \tag{3.35'}$$

The eigenvalue σ must be real because the operator on the right-hand side of Eqs. (3.35) is Hermitian. In accordance with this, we search for σ in the form

$$\sigma=q^2\sigma^{(2)}+\cdots \tag{3.37}$$

with a real $\sigma^{(2)}$. Insertion of Eqs. (3.35') and (3.37) into Eqs. (3.35) leads to the following equations for the functions $\tilde{r}_l^{(1)}(X)$:

$$\cos^2\theta_1(\tilde{r}_1^{(1)})''+(1-3r_1^2-gr_2^2)\tilde{r}_1^{(1)} -2gr_1r_2\tilde{r}_2^{(1)}\frac{\sin(2\theta_2)}{\sin(2\theta_1)}=-r_1'' , \tag{3.38a}$$

$$\cos^2\theta_2(\tilde{r}_2^{(1)})''+(1-3r_2^2-gr_1^2)\tilde{r}_2^{(1)} -2gr_2r_1\tilde{r}_1^{(1)}\frac{\sin(2\theta_1)}{\sin(2\theta_2)}=-r_2'' . \tag{3.38b}$$

Equations (3.38) must be supplemented by the boundary conditions

$$\tilde{r}_1^{(1)}=\tilde{r}_2^{(1)}=0 \quad \text{at } X\to\pm\infty$$

(we consider modes localized in the X direction transverse to the DB). The linear operator adjoint to that in the left-hand side of Eqs. (3.38) has the evident zero mode, viz. the row $(\sin(2\theta_1)r_1',\sin(2\theta_2)r_2')$. It is easy to see that the resolvability condition for the nonhomogeneous equations (3.38), requiring orthogonality of the right-hand side column $(-r_1'',-r_2'')$ to the zero-mode row, is fulfilled. At the second order in the small wave number q, the resolvability yields the following equation for the instability growth rate $\sigma^{(2)}$ [see Eq. (3.37)]:

$$\sigma^{(2)}=-\left[\int_{-\infty}^{+\infty}dX[(r_1')^2+(r_2')^2]\right]^{-1}\int_{-\infty}^{+\infty}dX[(r_1')^2\sin^2\theta_1+(r_2')^2\sin^2\theta_2+r_1'(\tilde{r}_1^{(1)})'\sin^2(2\theta_1)+r_2'(\tilde{r}_2^{(1)})'\sin^2(2\theta_2)] . \tag{3.39}$$

In particular, for the symmetric DB ($\theta_1=-\theta_2\equiv\theta$),

$$\sigma^{(2)}=-\sin^2\theta-\sin^2(2\theta)\frac{\int_{-\infty}^{+\infty}dX[r_1'(\tilde{r}_1^{(1)})'+r_2'(\tilde{r}_2^{(1)})']}{\int_{-\infty}^{+\infty}dX[(r_1')^2+(r_2')^2]} . \tag{3.40}$$

We have calculated the instability growth rate $\sigma^{(2)}$ for the above-mentioned cases $0<g-1\ll 1$ and $\theta_1=-\theta_2\equiv\theta$, $g=3$, in which the DB solution can be found in the explicit form. For the solution given by Eqs. (3.26) we find from Eqs. (3.38):

$$\tilde{r}_1^{(1)}(\xi)=\frac{1}{-\cos^2\theta}[-\tanh(\xi/2)-\xi\cosh\xi+(\sinh\xi)\ln 2 +(\sinh\xi)\ln(1+\cosh\xi)] , \tag{3.41a}$$

$$\tilde{r}_2^{(1)}(\xi)=-\tilde{r}_1^{(1)}(\xi), \quad \xi\equiv X\sqrt{2}/\cos\theta . \tag{3.41b}$$

Insertion of Eqs. (3.26) and (3.41) into Eq. (3.40) yields

$$\sigma^{(2)}=-(4\pi^2-39)\sin^2\theta<0 , \tag{3.42}$$

i.e., the DB given by Eq. (3.26) is stable against the long-wave distortions.

In the analytically tractable particular case (3.17) (we again confine ourselves to the symmetric DB, $\theta_1=-\theta_2\equiv\theta$), we employ the representation (3.18) and introduce the notation

$$\tau\equiv(g-1)T, \quad \xi\equiv\frac{\sqrt{g-1}X}{\cos\theta}, \quad \eta\equiv\frac{\sqrt{g-1}Y}{\cos\theta} \tag{3.43}$$

to deduce the following evolution equation for the phase function χ:

$$\chi_\tau=\chi_{\xi\xi}-\tfrac{1}{4}\sin(4\chi)+2\tan\theta[\sin(2\chi)\chi_\xi\chi_\eta-\cos(2\chi)\chi_{\xi\eta}] +(\tan^2\theta)\chi_{\eta\eta} . \tag{3.44}$$

On the background of the DB solution (3.23), we take a perturbation $\tilde{\chi}(\xi)\exp(iq\eta+\sigma\tau)$ which leads us to the eigenvalue problem

$$\sigma\tilde{\chi}=\tilde{\chi}_{\xi\xi}-\cos(4\chi)\tilde{\chi}+2iq\tan\theta[\sin(2\chi)\chi_\xi\tilde{\chi}-\cos(2\chi)\tilde{\chi}_\xi] -(\tan^2\theta)q^2\tilde{\chi} , \tag{3.45}$$

with the boundary condition $\tilde{\chi}(\xi\to\pm\infty)\to 0$. We find the following solution describing a long-wave distortion of the DB:

$$\tilde{\chi}=\operatorname{sech}\xi-iq(\tan\theta)(\operatorname{sech}\xi)\ln(\cosh\xi)+\cdots , \tag{3.46}$$

$$\sigma=-\tfrac{2}{3}(q\tan\theta)^2+\cdots , \tag{3.47}$$

cf. Eqs. (3.36), (3.37), (3.41), and (3.42). So, Eq. (3.47) tells us that the DB solution (3.23) is stable.

E. Domain boundary with a small "reflection angle"

1. General analysis

The case when the angle between the vectors $\mathbf{k}_1$ and $\mathbf{k}_2$ is small [see Fig. 1(a)] requires a special analysis. If this angle becomes $\lesssim\sqrt{\epsilon}$, the combinational wave vectors

$$\mathbf{k}_m \equiv \mathbf{k}_1 + (m-1)(\mathbf{k}_2 - \mathbf{k}_1) , \tag{3.48}$$

m being an integer, get to the instability range (2.3) or close to it. In this case, representation of a pattern in the form of the linear combination (2.4) of two families of the rolls ($N=2$) becomes irrelevant. Instead of this, one should base analysis on the single amplitude function $a(x,y,t)$, the Fourier transform of which comprises all the modes with the close wave vectors $\mathbf{k}_m$ [see Eq. (3.48)]. So, we assume that the wave vectors $\mathbf{k}_1$ and $\mathbf{k}_2$ can be represented in the form

$$\mathbf{k}_l = \mathbf{n} + \mathbf{q}_l, \quad l = 1,2 \tag{3.49}$$

where $\mathbf{n}$ is a unit vector, q_l are small. The aforementioned amplitude function is governed by the NWS equation [cf. Eqs. (2.5)]

$$a_t = \left[4 \left(\frac{\partial}{\partial x_1} - \frac{i}{2} \frac{\partial^2}{\partial y_1^2} \right)^2 + \epsilon \right] a - \kappa(0)|a|^2 a , \tag{3.50}$$

where

$$\frac{\partial}{\partial x_1} \equiv \cos\theta \frac{\partial}{\partial x} + \sin\theta \frac{\partial}{\partial y} ,$$

$$\frac{\partial}{\partial y_1} \equiv -\sin\theta \frac{\partial}{\partial x} + \cos\theta \frac{\partial}{\partial y} ,$$

and θ is the angle between the mean vector $\mathbf{n}$ [see Eq. (3.49)] and the x axis. The boundary conditions to Eq. (3.50) must be accorded with the definition (3.49):

$$\begin{aligned} &\frac{\nabla a}{a} \to i\mathbf{q}_1 \quad \text{at } x \to -\infty , \\ &\frac{\nabla a}{a} \to i\mathbf{q}_2 \quad \text{at } x \to +\infty , \end{aligned} \tag{3.51}$$

where ∇ stands for the gradient.

The description of DB can be reduced to an effectively one-dimensional problem in the only case when the vector $(\mathbf{k}_1 - \mathbf{k}_2)$ is parallel to the x axis. In the opposite case the problem is essentially two-dimensional, and the DB is, as a matter of fact, a linear array of dislocations.[11]

To illustrate the latter assertion, let us consider the simplest case when the vector $(\mathbf{k}_1 - \mathbf{k}_2)$ is parallel to the y axis (instead of the x axis);

$$\theta = 0, \quad (q_1)_y = -(q_2)_y \equiv q \ll 1 , \tag{3.52a}$$

$$(q_1)_x = (q_2)_x = -q^2/2 + O(q^4) , \tag{3.52b}$$

where the vectors $\mathbf{q}_1$ and $\mathbf{q}_2$ are defined according to Eq. (3.49) [Eq. (3.52b) provides $k_1^2 = k_2^2 = 1$]. In this case $x_1 = x$ and $y_1 = y$ in Eq. (3.50), and the boundary condition (3.51) takes the form

$$a \to \left(\frac{\epsilon}{\kappa(0)} \right)^{1/2} \exp[i(-\tfrac{1}{2}q^2 x \mp qy)] \quad \text{at } x \to \pm\infty . \tag{3.53}$$

Since the boundary condition (3.53) is periodic in y, we may search for periodic solutions:

$$a(x, y + 2\pi/q) = a(x,y) .$$

Symmetries of Eq. (3.50) guarantee existence of a periodic solution with the properties

$$\begin{aligned} &a(-x,y) = a^*(x,y) , \\ &a(x, y + \pi/q) = -a(x,y) . \end{aligned} \tag{3.54}$$

According to Eqs. (3.54), the function $a(0,y)$ is real, and it has at least two zeros per period at some points y_0 and $y_0 + \pi/q$. At these points, dislocations in the system of rolls are located: going round a dislocation gives rise to a change 2π of the phase of the complex amplitude $a(x,y)$.

2. Decay of a "one-dimensional" domain boundary

In a vicinity of a dislocation, the description of the dynamics of the system based on the amplitude equation (3.50) is irrelevant. However, the dynamics of dislocations, and dislocation-induced wave-number selection have been studied in detail in works quoted in Sec. I. That is why in the present work we confine ourselves to the dislocationless case, when the y components of the wave vectors $\mathbf{k}_1$ and $\mathbf{k}_2$ are equal: $(q_1)_y = (q_2)_y \equiv q_y$ [see Eq. (3.49)]. The substitution

$$a \equiv \left(\frac{\epsilon}{\kappa(0)} \right)^{1/2} B(X) e^{iq_y y} , \tag{3.55}$$

$$X = \tfrac{1}{2}\sqrt{\epsilon}x, \quad T \equiv \epsilon t \tag{3.56}$$

[cf. Eqs. (3.3b)] transform the boundary problem based on Eqs. (3.50) and (3.51) to the following form:

$$\begin{aligned} B_T = \Bigg\{ \Bigg[&\cos\theta \frac{\partial}{\partial X} + iQ_y \sin\theta \\ &- \frac{i}{4}\sqrt{\epsilon} \left(-\sin\theta \frac{\partial}{\partial X} + iQ_y \cos\theta \right)^2 \Bigg]^2 \\ &+ 1 \Bigg\} B - |B|^2 B , \end{aligned} \tag{3.57}$$

$$\begin{aligned} &\frac{1}{B}\frac{\partial B}{\partial X} \to \frac{2i}{\sqrt{\epsilon}} q_{1x} \quad \text{at } X \to -\infty , \\ &\frac{1}{B}\frac{\partial B}{\partial X} \to \frac{2i}{\sqrt{\epsilon}} q_{2x} \quad \text{at } X \to +\infty , \end{aligned} \tag{3.58}$$

where $Q_y \equiv 2q_y/\sqrt{\epsilon}$. The last term in the square brackets on the right-hand side of Eq. (3.57) may be neglected unless θ is close to $\pi/2$ (the case of θ close to $\pi/2$ is analyzed in Sec. III E 3). Then the change of variables

$$B \equiv A \exp[-iQ_y(\tan\theta)X], \quad X \equiv X'\cos\theta \tag{3.59}$$

transforms Eqs. (3.57) and (3.58) into the form

$$A_T = A_{X'X'} + (1-|A|^2)A \ , \tag{3.60}$$

$$\frac{A_{X'}}{A} \to iK_{\pm} \quad \text{at } X' \to \pm\infty \ , \tag{3.61}$$

where

$$K_- \equiv \mathbf{Q}_1 \cdot \mathbf{n}, \quad K_+ \equiv \mathbf{Q}_2 \cdot \mathbf{n}, \quad \mathbf{Q}_{1,2} \equiv 2\mathbf{q}_{1,2}/\sqrt{\epsilon} \ . \tag{3.62}$$

At last, setting $A \equiv r\exp(i\varphi)$ and $K \equiv \varphi_{x'}$ brings Eqs. (3.60) and (3.61) to the final form:

$$r_T = r_{X'X'} + r(1-K^2-r^2) \ , \tag{3.63a}$$

$$K_T = [r^{-2}(r^2K)_{X'}]_{X'} \ , \tag{3.63b}$$

$$K \to K_{\pm} \quad \text{at } X' \to \pm\infty \ . \tag{3.64}$$

As is well known, all stationary solutions of the system of equations (3.63) can be found analytically (see, e.g., Ref. 34). The only stable solutions are

$$r^2 = 1-K^2, \quad K = \text{const} \quad (K^2 < 1) \tag{3.65}$$

(the stability requires[15] $K^2 < \frac{1}{3}$). There are no stationary solutions satisfying the boundary conditions (3.64) with $K_+ \neq K_-$. It is easy to see that traveling-wave solutions do not exist either. Indeed, insertion of

$$r = r(X'-cT), \quad K = K(X'-cT) \ ,$$

into Eq. (3.63b) yields the equation

$$K'_{\xi} + 2(r'_{\xi}/r)K + cK = \text{const}, \quad \xi \equiv X'-cT \ ,$$

which is incompatible with Eq. (3.64) of $K_+ \neq K_-$.

So, the one-dimensional boundary problem based on Eqs. (3.63) and (3.64) has no DB-like stationary solutions. Numerical simulations[30] demonstrate that a DB-like initial configuration spreads and smooths down at large times, provided the initial state contains no unstable region with $K^2 > \frac{1}{3}$. In the course of the system's evolution, the function $r(X')$ vanishes nowhere, hence the quantity $\int_{-\infty}^{+\infty} dX' K(X')$, proportional to a total number of convection rolls in the system, is conserved according to Eq. (3.63b). It is relevant to note that, if the initial configuration contains unstable regions (with $K^2 > \frac{1}{3}$), the unstable pattern will be supplanted by a stable one with change of the total number of rolls.[29]

The process of spreading and smoothing down of an initial DB-like configuration can be described analytically in the so-called geometric optics approximation[35,36] if a characteristic size δ^{-1} of the initial profile $r_0(X')$ and $K_0(X')$ is large (as compared to the roll's size k_c^{-1} equal to unity in our designation). Let us introduce the new independent variables $\Xi \equiv X'\delta$, $\tau \equiv T\delta^2$, and expand a solution in powers of δ. At the lowest order one obtains from Eqs. (3.63) the following equations:[30,35]

$$r(1-K^2-r^2) = 0 \ , \tag{3.66a}$$

$$K_{\tau} = K_{\Xi\Xi} + 2(r^{-1}r_{\Xi}K)_{\Xi} \ . \tag{3.66b}$$

Inserting the solution of Eq. (3.66a), $r = 1-K^2$, into Eq. (3.66b), we arrive at the nonlinear phase diffusion equation:

$$K_{\tau} = [D(K)K_{\Xi}]_{\Xi} \ , \tag{3.67a}$$

where

$$D(K) \equiv (1-3K^2)/(1-K^2) \tag{3.67b}$$

is the nonlinear diffusion coefficient. Note that the stability condition $D(K) \geq 0$, i.e., $K^2 \leq \frac{1}{3}$, for the stationary solutions $K = \text{const}$ ensuing from the approximate phase diffusion equation (3.67) coincides with the stability condition following from the exact equations (3.63).

Let us consider evolution of a profile $K(\Xi)$ of the form $K(\Xi) = K_-$ at $\Xi < \Xi_-$, $K(\Xi) = K_+$ at $\Xi > \Xi_+$, and some smooth function interpolates between K_+ and K_- (we assume $K_{\pm}^2 \leq \frac{1}{3}$). A straightforward calculation with Eq. (3.67a) gives

$$\frac{d}{d\tau}\int_{\Xi_-}^{\Xi_+} K_{\Xi}^2 d\Xi = -2\int_{\Xi_-}^{\Xi_+} D(K)K_{\Xi\Xi}^2 d\Xi + \tfrac{2}{3}\int_{\Xi_-}^{\Xi_+} D''(K)K_{\Xi}^4 d\Xi \ . \tag{3.68}$$

As $D''(K) = -4(1-K^2)^{-3}(3+K^2) < 0$ [see Eq. (3.67b)], the right-hand side of Eq. (3.68) is negative. Equation (3.68), together with the evident fact that the size $(\Xi_+ - \Xi_-)$ of the transient layer grows with time, tell us that a mean value of K_{Ξ}^2 in the transient layer decreases monotonically, i.e., the DB-like pattern (transient layer) smooths down indeed.

An asymptotic stage of spreading of the DB-like pattern governed by Eq. (3.67) is described by a self-similar solution of the form $K = K(z)$, $z \equiv \Xi/\sqrt{\tau}$. This solution is determined by the boundary problem

$$[D(K)K'_z]'_z + \tfrac{1}{2}zK'_z = 0 \ , \tag{3.69}$$

$$K \to K_{\pm} \quad \text{at } z \to \pm\infty \ . \tag{3.70}$$

At $z \to \pm\infty$ the self-similar solution demonstrates the asymptotic behavior

$$K - K_{\pm} \sim z^{-1}\exp[-z^2/4D(K_{\pm})] \ . \tag{3.71}$$

In the limit $K_{\pm}^2 \ll 1$, Eq. (3.69) may be linearized:

$$K'_{zz} + \tfrac{1}{2}zK'_z = 0 \ . \tag{3.69'}$$

The solution of the linear boundary problem based on Eqs. (3.69') and (3.70) can be found right away:

$$K(z) = \tfrac{1}{2}(K_+ + K_-) + \tfrac{1}{2}(K_+ - K_-)\text{sgn}(z)\text{erf}(2z) \ ,$$

where $\text{erf}(x)$ is the standard integral of probabilities.

Numerical solutions of the full nonlinear boundary problem (3.69) and (3.70) for the case $K_- = -K_+$ [in this case $K(-z) = -K(z)$] are shown in Fig. 4. According to Eqs. (3.71) and (3.67b), the approach of $K(z)$ to K_+ at $z \to +\infty$ becomes faster with the growth of K_+. At $K_+ = 1/\sqrt{3}$ (recall this is a boundary of the stability range for the solutions $K = \text{const}$), the graph $K(z)$ becomes broken (see Fig. 4): It is easy to obtain from Eq. (3.69) that at the breaking point ($Z = Z_*$, see Fig. 4)

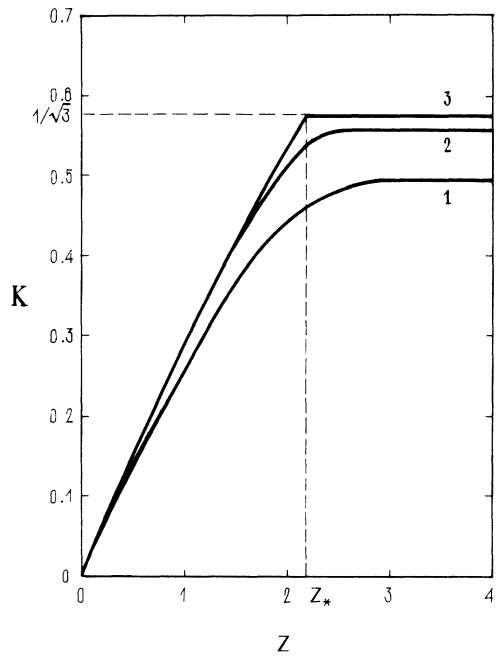

FIG. 4. The self-similar solutions $K(z)$, $z \equiv \Xi/\sqrt{\tau}$, of the nonlinear phase diffusion equation (3.67) with the boundary conditions $K_- = -K_+$ [in this case the function $K(z)$ is odd, that is why only positive z are shown]. The graphs 1, 2, and 3 correspond to $K_+ = 0.5004$, $K_+ = 0.5603$, and $K_+ = 1/\sqrt{3}$, respectively.

$\lim_{z - z_* \to -0} dK/dz = z_*/6\sqrt{3}$, while $K \equiv K_+$ at $z - z_* > 0$. The numerical calculation gives $z_* \approx 2.18$.

3. *Stable symmetric domain boundary*

In the special case $\theta = \pi/2$ the rolls are nearly perpendicular to the DB [see Eq. (3.49) and Fig. 5]. In this case,

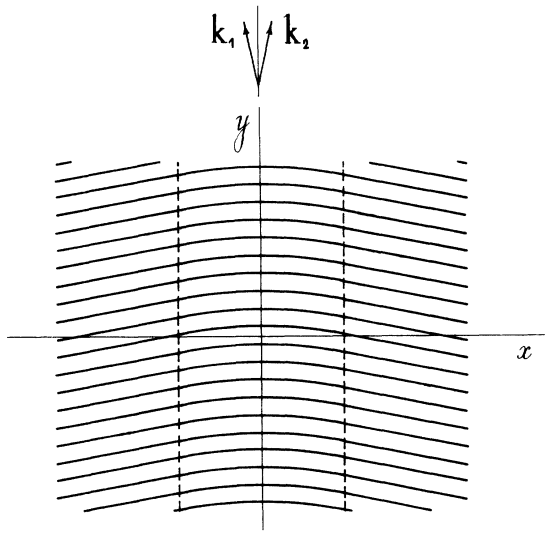

FIG. 5. The symmetric domain boundary in the case of a small "refraction angle" and $\theta = \pi/2$.

it is natural to define the "slow coordinate" as

$$X = \epsilon^{1/4} x \ , \tag{3.72}$$

instead of Eq. (3.56) in the general case ($\theta \neq \pi/2$). We set, as above, $(q_1)_y = (q_2)_y \equiv q_y$, and define the slow time T according to Eq. (3.56) and the amplitude $a(T,X)$ according to Eq. (3.55). In this notation, Eqs. (3.57) and (3.58) take the form

$$B_T = \left[-\left(\frac{\partial^2}{\partial X^2} - Q_y \right)^2 + 1 \right] B - |B|^2 B \ , \tag{3.73}$$

$$B_X / B \to i K_\pm \quad \text{at } X \to \pm\infty \ , \tag{3.74}$$

where $K_- \equiv (q_1)_x \epsilon^{-1/4}$, $K_+ \equiv (q_2)_x \epsilon^{-1/4}$, and, as above, $Q_y \equiv 2 q_y / \sqrt{\epsilon}$.

The dynamics of weakly curved rolls (Fig. 5) governed by Eqs. (3.73) and (3.74) strongly depend on the ratios $Q_y / K_\pm$. As is well known, the homogeneous roll patterns with $k < 1$ are unstable against the so-called zigzag perturbations (long-wave transverse distortions).[15] According to Eq. (3.49), for the two homogeneous patterns matched by the DB the corresponding stability conditions $k_{1,2} \geq 1$ are $Q_y + K_\pm^2 \geq 0$. As will be demonstrated below, a stationary DB is possible only at the boundary of the zigzag stability range, viz., at $K_\pm = \pm(|Q_y|)^{1/2}$, $Q_y < 0$. This DB is obviously symmetric (see Fig. 5).

In the subsequent analysis, we confine ourselves to the case $|K_\pm| \ll 1$, when the phase-dynamics approximation[37] [an example of which is Eq. (3.67)] is applicable. Assuming $Q_y < 0$, $Q_y \sim K_\pm^2$, we define the new coordinate $\xi \equiv (|Q_y|)^{1/2} X$ to bring Eqs. (3.73) and (3.74) to the form

$$B_T = -Q_y^2 \left(\frac{\partial^2}{\partial \xi^2} + 1 \right)^2 B + (1 - |B|^2) B \ , \tag{3.75}$$

$$B_\xi / B \underset{\xi \to \pm\infty}{\to} i Q_\pm, \quad Q_\pm \equiv K_\pm / (|Q_y|)^{1/2} \ . \tag{3.76}$$

Inserting the expansion $B = B_0 + Q_y^2 B_1 + \cdots$ into Eq. (3.75) yields, at the lowest order,

$$B_0 = \exp(i\varphi) \tag{3.77}$$

(i.e., $|B_0| = 1$), and the well-known Cahn-Hilliard equation[38]

$$Q_\tau + \frac{\partial^2}{\partial \xi^2} (Q_{\xi\xi} + 2Q - 2Q^3) = 0, \quad Q \equiv \varphi_\xi \ , \tag{3.78}$$

at the next order. In Eq. (3.78), $\tau \equiv Q_y^2 t$. It is well known (see, e.g., Ref. 39) that the only stable stationary solution of the CH equation (3.78) is the kink

$$Q = \pm \tanh \xi \ . \tag{3.79}$$

According to Eq. (3.77), the solution (3.79) describes the DB of the form

$$B = \exp(\pm i \ln\{\cosh[(|Q_y|)^{1/2} X]\}) \tag{3.80}$$

(shown in Fig. 5), provided it satisfies the boundary conditions (3.76), i.e., if $Q_\pm = \pm 1$ or $Q_\pm = \mp 1$. According to Eq. (3.76), this means

$$K_+ = -K_- = \pm(|Q_y|)^{1/2} \ .$$

The DB solution (3.80) is stable. Its stability against one-dimensional perturbations is a well-known result of the theory of the CH equation.[41,38] To study two-dimensional perturbations, one needs a two-dimensional generalization of Eq. (3.78) for the phase φ. This equation can be deduced, in the geometric optics approximation, from the full two-dimensional amplitude equation obtained from Eq. (3.73) by means of the substitution $Q_y \to -i(\partial/\partial Y)$, $Y \equiv \frac{1}{2}\sqrt{\epsilon}y$ [cf. Eq. (3.72)]. The resultant phase evolution equation is

$$\varphi_T + \varphi_{XXXX} - \varphi_{YY} - 2\varphi_Y \varphi_{XX} - 4\varphi_X \varphi_{XY} - 6\varphi_X^2 \varphi_{XX} = 0 \ . \tag{3.81}$$

Analysis of two-dimensional perturbations in the form of long-wave distortions of the DB can be readily performed in the framework of Eq. (3.81). As a result, we find that the perturbations decay $\sim \exp(-\tilde{Q}_y^2 T)$, $\tilde{Q}_y$ being a small wave number of the perturbation.

Our general conclusion is that, as a rule, stationary DB's are not possible in a system of almost parallel rolls. The symmetric DB configuration shown in Fig. 5 and described analytically by the solution (3.80) is the only exception.

IV. DOMAIN BOUNDARIES BETWEEN HEXAGONS AND ANOTHER PATTERN

A. Formulation of the problem

In this section we consider DB's in the system governed by Eqs. (2.5) in the presence of the resonant interaction, i.e., at $\alpha \neq 0$. As is well known,[18] in this case the hexagonal pattern is stable at $|\epsilon| \lesssim \alpha$ (including negative ϵ), and the stability range of the hexagons overlaps with those of both the rolls (at $\epsilon > 0$) and the quiescent state (at $\epsilon < 0$).

In accordance with this, at $\epsilon < 0$ a solution of Eqs. (2.5) singled out by the boundary conditions

$$\begin{aligned} &|a_1| = |a_2| = |a_3| \equiv a_h \neq 0 \quad \text{at } x = -\infty \ , \\ &a_l = 0 \quad \text{at } x = +\infty, \ l = 1,2,3 \end{aligned} \tag{4.1}$$

corresponds to DB of the hexagon–quiescent-state type, see Fig. 1(b) [recall it is implied that $\mathbf{k}_1 + \mathbf{k}_2 + \mathbf{k}_3 = 0$ in Eqs. (2.5)].

At $\epsilon > 0$, the DB of the hexagon-roll type [Fig. 1(c)] is specified by the boundary conditions

$$\begin{aligned} &|a_1| = |a_2| = |a_3| \equiv a_h \neq 0 \quad \text{at } x = -\infty \ , \\ &|a_1| \equiv a_r \neq 0, \ a_2 = a_3 = 0 \quad \text{at } x = +\infty \ . \end{aligned} \tag{4.2}$$

The DB of a more general form is possible in a pattern composed of four systems of rolls [$N=4$ in Eq. (2.4)], provided three of them are related by the resonance equation $\mathbf{k}_1 + \mathbf{k}_2 + \mathbf{k}_3 = 0$. The DB solution satisfies the boundary conditions

$$\begin{aligned} &|a_1| = |a_2| = |a_3| \equiv a_h \neq 0, \quad a_4 = 0 \quad \text{at } x = -\infty \ , \\ &a_1 = a_2 = a_3 = 0, \quad |a_4| \equiv a_r \neq 0 \quad \text{at } x = +\infty \ . \end{aligned} \tag{4.3}$$

In either case $\epsilon \gtrless 0$, a DB between hexagonal patterns based on resonance triads with different orientations is possible too, but we will not consider this type of DB as it gives rise to cumbersome systems of equations and does not seem to be of a substantial practical interest.

At last, in the case $\epsilon > 0$ the "resonant" DB between two systems of rolls, the angle between the wave vectors of which is $2\pi/3$ or $\pi/3$ [Fig. 1(d)], can be considered. In this case, the resonant interaction generates a strip of hexagons sandwiched between the two roll patterns [see Fig. 1(d)], so that the resonant DB is, as a matter of fact, a bound state of two DB's of the hexagon-roll type. The corresponding boundary conditions are

$$\begin{aligned} &|a_1| = a_r \neq 0, \quad a_2 = a_3 = 0 \quad \text{at } x = -\infty \ , \\ &|a_2| = a_r \neq 0, \quad a_1 = a_3 = 0 \quad \text{at } x = +\infty \ . \end{aligned} \tag{4.4}$$

B. "Hexagon–quiescent-state" and "hexagon-roll" domain boundaries

1. Preliminaries

In the subsequent analysis we confine ourselves to the case when all the wave numbers k_l ($l=1,2,3$) far from the DB are equal to $k_c \equiv 1$. In this case, the amplitudes a_l in Eqs. (2.5) may be assumed real. The scale transformation

$$a_l \equiv \frac{\alpha}{\kappa(0)} A_l, \quad T \equiv \frac{\alpha^2}{\kappa(0)} t, \quad X \equiv \frac{\alpha}{2\sqrt{\kappa(0)}} x \tag{4.5}$$

brings Eq. (2.5) into the form

$$\begin{aligned} (A_1)_T = D_1 (A_1)_{XX} + [\gamma - A_1^2 - g(A_2^2 + A_3^2)] A_1 \\ + A_2 A_3 \ , \end{aligned} \tag{4.6}$$

and two other equations are obtained from Eq. (4.6) by cyclic permutations of the indices (1,2,3). Here we have introduced the notations

$$D_l \equiv (k_l)_x^2, \quad \gamma \equiv \epsilon\kappa(0)/\alpha^2, \quad g \equiv \kappa(\pi/3)/\kappa(0) \ . \tag{4.7}$$

Equations (4.6) and (4.7) have been deduced earlier in Ref. 14. In the same work, the problem of finding the DB of the hexagon-roll type has been formulated, but not solved.

The homogeneous hexagonal and roll patterns are given, respectively, by the following evident solutions to Eq. (4.6):

$$A_1 = A_2 = A_3 \equiv A_h = \frac{1 + \sqrt{1 + 4\gamma(1+2g)}}{2(1+2g)} \ , \tag{4.8}$$

$$A_2 = A_3 = 0, \quad A_1 \equiv A_r = \gamma^{1/2} \ . \tag{4.9}$$

It is well known[17,18] that, within the framework of Eqs. (4.6), the stability ranges of the solutions (4.8) and (4.9) are, respectively,

$$-\frac{1}{4(1+2g)} \leq \gamma \leq \frac{g+2}{(g-1)^2} \ , \tag{4.10}$$

$$\gamma \geq (g-1)^{-2} \tag{4.11}$$

(recall we assume $g - 1 > 0$, otherwise the rolls are unsta-

ble). As it follows from Eqs. (4.10) and (4.11), the two stability ranges overlap indeed in the region

$$(g-1)^{-2} \leq \gamma \leq (g+2)(g-1)^{-2} . \tag{4.12a}$$

On the other hand, in the region

$$-\tfrac{1}{4}(1+2g)^{-1} \leq \gamma < 0 \tag{4.12b}$$

both the hexagons and the quiescent state, corresponding to the trivial solution $A_1 = A_2 = A_3 = 0$, are stable.

2. *Hexagon–quiescent state*

Now we proceed to x-dependent solutions of Eqs. (4.6). Let us designate $\theta_1 \equiv \theta$ ($|\theta| \leq \pi/2$), then

$$\begin{aligned} D_1 &= \cos^2\theta , \\ D_2 &= \tfrac{1}{4}(\cos\theta - \sqrt{3}\sin\theta)^2 , \\ D_3 &= \tfrac{1}{4}(\cos\theta + \sqrt{3}\sin\theta)^2 . \end{aligned} \tag{4.13}$$

An immobile DB between the hexagons and the quiescent state is possible at a single value of the parameter γ. Indeed, the stationary versions ($\partial/\partial T = 0$) of Eqs. (4.6) are nothing but equations of motion for a mechanical system with the Lagrangian [cf. Eqs. (3.15) and (3.16)]

$$L = \sum_{l=1}^{3} \tfrac{1}{2} D_l (A_l')^2 - U , \tag{4.14}$$

$$U = \sum_{l=1}^{3} \left[\tfrac{1}{2}\gamma A_l^2 - \tfrac{1}{4} A_l^4 - \frac{g}{2}(A_1^2 A_2^2 + A_1^2 A_3^2 + A_2^2 A_3^2) \right] + A_1 A_2 A_3 , \tag{4.15}$$

the prime standing for d/dX (the coordinate X plays the role of time). The immobile DB corresponds to a separatrix trajectory of the mechanical system which connects the local maximum of the effective potential (4.15) corresponding to the hexagonal pattern (4.8) and the trivial extremum $A_1 = A_2 = A_3 = 0$ corresponding to the quiescent state. Evidently, this separatrix cannot exist unless the values of the potential U at the two points are equal. A straightforward calculation demonstrates that it is possible at

$$\gamma = \gamma_1 \equiv -\frac{2}{9(1+2g)} . \tag{4.16}$$

The physical meaning of this result is clear: As well as in the roll-roll problem, the effective Lagrangian (4.14) coincides with the density of the Lyapunov functional (2.6b). The DB may be immobile only if the Lyapunov densities for the two patterns matched via the DB are equal. At last, for the homogeneous patterns $L = -U$ according to Eq. (4.14).

The linear density of the Lyapunov functional (2.6b)

$$\mathcal{F}(\theta) \equiv \int_{-\infty}^{+\infty} dX [L(X) - L(\infty)]$$

for the immobile DB may be found numerically, as we could not find any analytical solution of the problem (4.1), (4.6), (4.13). For instance, in the case $g \equiv 2$ (which corresponds to the Swift-Hohenberg model with an additional quadratic term taking account of the resonant interaction[40]) our numerical computations have demonstrated that $\mathcal{F}(\theta) \approx 0.011$ is practically independent of the angle θ.

If $\gamma \neq \gamma_1$, Eqs. (4.6) with the boundary conditions (4.1) have a solution in the form of a DB moving with a constant velocity c: $A_l = A_l(\xi)$, $\xi \equiv X - cT$. The functions $A_l(\xi)$ are determined by the equations

$$D_1 A_1'' + c A_1' + A_1[\gamma - A_1^2 - g(A_2^2 + A_3^2)] + A_2 A_3 = 0 \tag{4.17a}$$

(and two other equations obtained by the permutations of the indices), which are the aforementioned mechanical equations of motion supplemented by the dissipative terms (friction forces) cA_l'. It is straightforward to see that the DB moves to the right if $L(-\infty) < L(+\infty)$, and to the left in the opposite case, i.e., in accordance with the relation (2.6a), a pattern with the smaller value of the Lyapunov density supplants that with the larger density. This situation is similar to the motion of a front of an off-equilibrium phase transition of the first order (see, e.g., Ref. 41). Equations (2.7) and (2.6b) give rise to the following general expression for the DB's velocity:

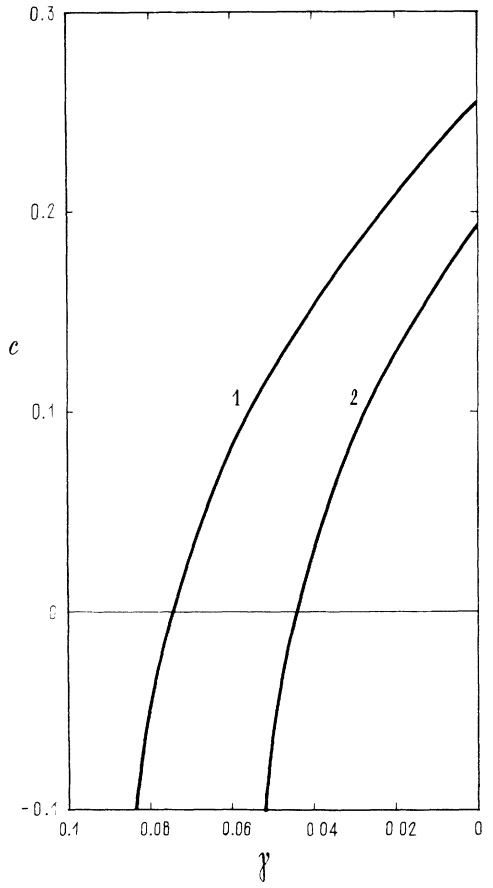

FIG. 6. The velocity of the domain boundary between hexagons and the quiescent state at $\theta = 0$ and two different values of g: (1) $g = 1$; (2) $g = 2$.

$$c=(L_1-L_2)\Big/\sum_l \int_{-\infty}^{+\infty} dX[(A_l)_X]^2 , \tag{4.17b}$$

where L_1 and L_2 stand for the Lyapunov densities (Lagrangians in the equivalent mechanical problem) of the, respectively, "less favorable" (supplanted) and "more favorable" (supplanting) patterns matched via the moving DB. In particular, at small $|\gamma-\gamma_1|$ one may calculate the denominator in Eq. (4.17b) using the form of $A_l(x)$ at $\gamma=\gamma_1$. Evidently, in this case $c=\text{const}\times(\gamma-\gamma_1)+O[(\gamma-\gamma_1)^2]$ (the Onsager regime).

In Fig. 6 we display dependences $c(\gamma)$ obtained by numerically solving Eq. (4.17a). We have depicted the dependences for $\theta=0$, but our numerical results demonstrate that a dependence $c(\theta)$ at a fixed γ, i.e., the effective anisotropy of the DB, is extremely weak: When θ changes inside its range of definition $-\pi/2\le\theta\le\pi/2$, c changes by not more than 0.3% of its mean value.

3. *Hexagon-roll*

This DB is specified by the boundary conditions (4.2). The DB is immobile at

$$\gamma=\gamma_2\equiv\frac{2(1+3g)+[2(1+g)]^{3/2}}{4(1+2g)(g-1)^2} \tag{4.18}$$

[cf. Eq. (4.16)]. At $\gamma=\gamma_2$ and small $(g-1)$ [cf. Eq. (3.17)] a corresponding analytical solution of the stationary version of Eqs. (4.6) can be obtained in the cases $\theta=0$ (the rolls parallel to the DB) and $\theta=\pi/2$ (the rolls perpendicular to the DB), where the angle θ is defined in Fig. 1(c). In both cases it follows from Eqs. (4.13) that $D_2=D_3$, hence Eqs. (4.6) admit the reduction $A_2=A_3$. To transform Eqs. (4.6) into a more suitable form, we employ the substitution

$$A_1\equiv\frac{2}{\sqrt{3}}\frac{r\cos\chi}{g-1},\quad A_2=A_3\equiv\left[\frac{2}{3}\right]^{1/2}\frac{r\sin\chi}{g-1} , \tag{4.19}$$

$$Z\equiv\frac{2}{\sqrt{3(g-1)}}X . \tag{4.20}$$

It is easy to find that $r=1+O(g-1)$ [cf. Eq. (3.19b)]. At $\theta=0$, the equation for χ and the corresponding boundary condition take the form

$$\frac{d\chi}{dZ}=\sin\chi\frac{1-\sqrt{3}\cos\chi}{(4-3\cos^2\chi)^{1/2}} , \tag{4.21}$$

$$\chi\to\cos^{-1}(1/\sqrt{3})\ \text{ at } Z\to-\infty ,\qquad \chi\to0\ \text{ at } Z\to+\infty \tag{4.22}$$

[cf. Eqs. (3.20) and (3.21)]. The solution of the boundary problem (4.21) and (4.22) can be written in the implicit form [cf. Eqs. (3.22) and (3.23)]:

$$Z-Z_0=\frac{\sqrt{3}-1}{4}\ln\frac{4+3\cos\chi+(4-3\cos^2\chi)^{1/2}}{1+\cos\chi}+\frac{\sqrt{3}+1}{4}\ln\frac{4-3\cos\chi+(4-3\cos^2\chi)^{1/2}}{1-\cos\chi}$$
$$-\tfrac{3}{2}\ln\frac{\frac{4}{\sqrt{3}}-\cos\chi+(4-3\cos^2\chi)^{1/2}}{\sqrt{3}\cos\chi-1} . \tag{4.23}$$

Quite analogously, in the case $\theta=\pi/2$ the equation for χ is [cf. Eq. (4.21)]

$$\frac{d\chi}{dZ}=\frac{1}{\sqrt{3}}(1-\sqrt{3}\cos\chi)\tan\chi , \tag{4.24}$$

and its implicit solution is [cf. Eq. (4.23)]

$$Z-Z_0=\frac{\sqrt{3}}{4}[(\sqrt{3}-1)\ln(1+\cos\chi)-(\sqrt{3+1})\ln(1-\cos\chi)]+\frac{\sqrt{3}}{2}\ln\left[\cos\chi-\frac{1}{\sqrt{3}}\right] . \tag{4.25}$$

We have developed numerical analysis of the boundary problem determining the DB hexagon-roll in the general (nonintegrable) case. The numerically computed dependence of the DB's linear density $\mathcal{F}(\theta)$ of the Lyapunov functional (2.6b) upon the angle θ is weak (Fig. 7). At $\gamma\neq\gamma_2$, the dependence of the velocity c of the moving DB upon the angle θ is sufficiently weak too (see Figs. 8 and 9).

At last, it is possible to consider the DB hexagon-roll of a more general type, when the superposition (2.4) involves four different wave vectors $\mathbf{k}_l$, three of them being resonantly coupled. Numerical analysis of the corresponding system of coupled Ginzburg-Landau equations analogous to Eq. (4.6) has yielded a noticeable qualitative result: In the case $\gamma\neq\gamma_2$ the DB's velocity c proves to be appreciably smaller than in the problem involving three modes. Another noteworthy qualitative result of the numerical analysis is the fact that, among the three resonantly coupled amplitudes, only the one with the largest diffusion coefficient D_l defined according to Eq. (4.7) varies monotonically, while the others may have a maximum (Fig. 10).

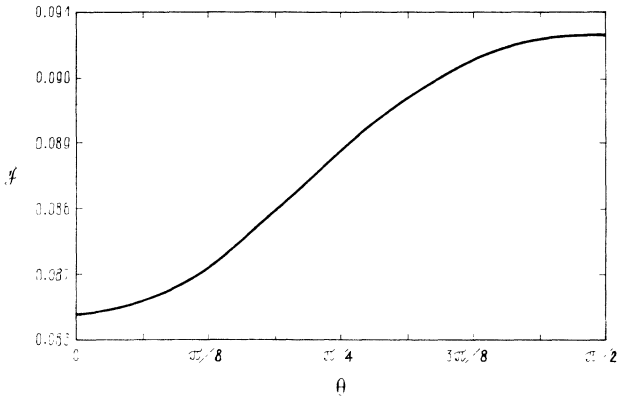

FIG. 7. The linear density of the Lyapunov functional for the DB hexagon-roll vs its orientation angle θ at $\gamma=\gamma_2$, $g\equiv 2$.

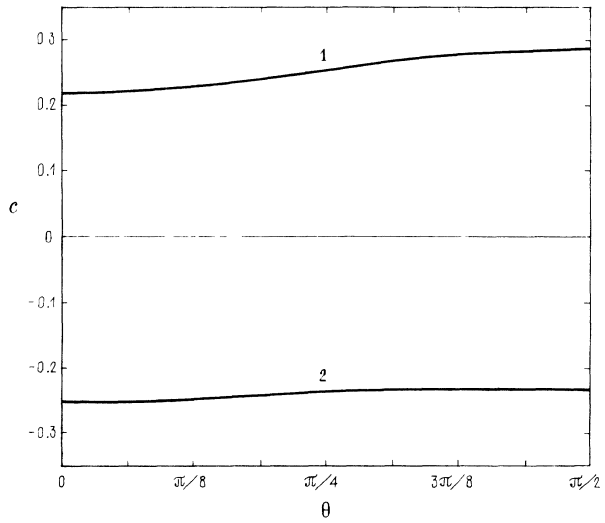

FIG. 9. The dependence of the velocity c of the DB hexagon-roll upon the orientation angle θ for different values of γ: (1) $\gamma=1$; (2) $\gamma=2$ (in both cases, $g\equiv 2$).

C. Pinning of a domain boundary by the small-scale structure

1. General analysis

The previous consideration has been developed in the framework of Eqs. (2.5) for the envelope amplitudes ignoring a direct influence of the underlying small-scale structure of the roll or hexagonal pattern. As is known, the small-scale structure may give rise to exponentially weak nonadiabatic effects which cannot be accounted for by the amplitude equation that governs large-scale modulation of a pattern. In Ref. 14, Pomeau has conjectured that the nonadiabatic interaction of a moving front (DB) with the small-scale structure may give rise to pinning of the DB by the structure via a process of adjusting the structure's wave number. It is also relevant to mention Ref. 42, where the problem of pinning of a DB-like front by an underlying small-scale structure was discussed for patterns produced by oscillatory convection.

In this subsection we will demonstrate that the pinning of the moving DB's involving the hexagonal pattern is possible indeed, provided the DB is nearly perpendicular

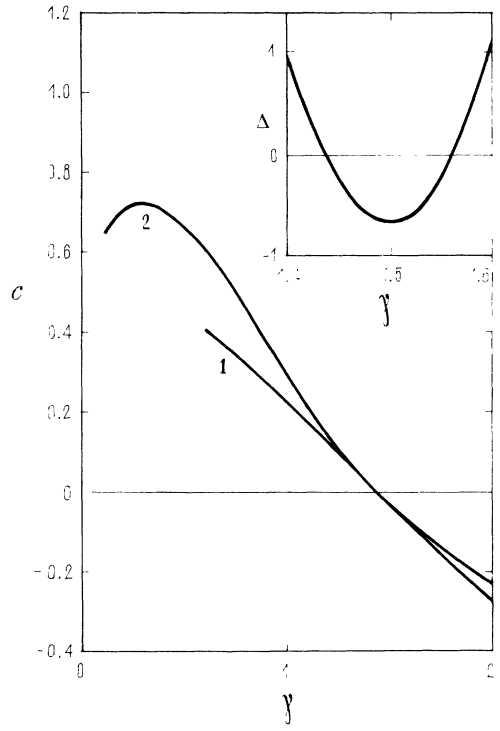

FIG. 8. The velocity of the moving DB hexagon-roll vs the parameter γ at $g=2$. The curves 1 and 2 pertain, respectively, to $\theta=0$ and $\theta=\pi/2$. To illustrate how weak is the orientation dependence of the velocity, in the inset we show the difference $\Delta\equiv[c(\pi/2)-c(0)]10^3$ vs γ in a vicinity of $\gamma=\gamma_2$.

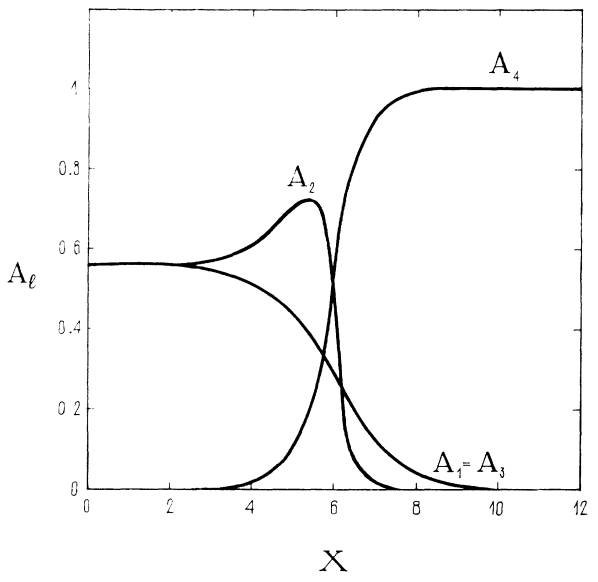

FIG. 10. A typical example of a numerical solution for the DB interpolating between the hexagons based on the wave vectors $\mathbf{k}_1,\mathbf{k}_2,\mathbf{k}_3$ ($\mathbf{k}_1+\mathbf{k}_2+\mathbf{k}_3=0$) and rolls based on a different wave vector $\mathbf{k}_4$; $\gamma=1$, $g\equiv 2$, $\theta=\pi/6$. The angle between the wave vector $\mathbf{k}_4$ and the x axis is $\pi/3$.

to any of the wave vectors $\mathbf{k}_l$ on which the hexagons are based. This pinning requires no change (adjusting) of the underlying wave number.

A direct analysis of the pinning effect starting from the hydrodynamic equations of the convection theory is extremely tedious. That is why we will base our analysis on the phenomenological Swift-Hohenberg (SH) model[43] modified by adding the quadratic term into the equation of motion.[40] Then we will demonstrate that an estimate for an exponentially small strength of pinning obtained for the modified SH model has quite a general character and does not depend on details of nonlinear coupling of modes.

In an appropriate notation, the modified SH model takes the form

$$\psi_t=\epsilon\gamma\psi-\tfrac{1}{4}(\nabla^2+1)^2\psi+\sqrt{\epsilon}\psi^2-\tfrac{1}{3}\psi^3 , \tag{4.26}$$

where ∇^2 stands for the two-dimensional Laplacian. As above, ϵ is the small overcriticality (we assume it positive), and $\gamma\sim\epsilon/\alpha^2$ [see Eqs. (4.7)], where α is the small resonance coupling constant (the case $\gamma\sim 1$ is of main interest). The DB between hexagons and rolls is described by the expression

$$\psi=2\sqrt{\epsilon}\sum_{l=1}^{3} A_l(\sqrt{\epsilon}x,\epsilon t)\cos(\mathbf{k}_l\cdot\mathbf{r})+O(\epsilon) , \tag{4.27}$$

where the amplitudes A_l are governed by the coupled Ginzburg-Landau equations (4.6) [with regard to Eqs. (4.5)] with $g\equiv 2$. For the time being, we confine ourselves to the case $\theta=0$, i.e., $D_1=1$, $D_2=D_3=\frac{1}{4}$, and $A_2=A_3$. The DB is immobile at $\gamma=\gamma_1=-\frac{2}{45}$ and at $\gamma=\gamma_2=(7+3\sqrt{6})/10$. Of course, the expression (4.27) is not an exact solution to Eq. (4.26), even if the amplitudes A_l are exact solutions to Eqs. (4.6). Let us look for a corrected solution at small $|\gamma-\gamma_2|$ in the form

$$\psi=\psi_0+\psi_1+\tilde{\psi} , \tag{4.28}$$

where

$$\psi_0=2\sqrt{\epsilon}\sum_{l=1}^{3} A_l(\sqrt{\epsilon}[x-\xi(\epsilon t)])\cos(\mathbf{k}_l\cdot\mathbf{r}) , \tag{4.29}$$

cf. Eq. (4.27), ψ_1 is a contribution from higher-order corrections to the amplitude equations, which is a series in powers of $\epsilon^{1/2}$, and $\tilde{\psi}$ takes its origin in nonadiabatic effects and, also, takes account of a small difference on γ from γ_2. Direct insertion of Eq. (4.29) into the underlying evolution equation (4.26) leads to the following linearized equation for $\tilde{\psi}$:

$$\epsilon\gamma_2\tilde{\psi}-\tfrac{1}{4}(\nabla^2+1)^2\tilde{\psi}+2\sqrt{\epsilon}\psi_0\tilde{\psi}-\psi_0^2\tilde{\psi} = \frac{\partial\psi_0}{\partial\xi}\frac{d\xi}{dt}-\epsilon(\gamma-\gamma_2)\psi_0-G , \tag{4.30}$$

where G is an expression containing a fast dependence on $\mathbf{r}$ of the type $\cos(\mathbf{k}_n\cdot\mathbf{r})$, which is a source of the nonadiabaticity. An explicit form of G is rather cumbersome. The linear operator of the left-hand side of Eq. (4.30) has the zero eigenmode $\partial\psi_0/\partial\xi$, hence the resolvability of Eq. (4.30) requires the orthogonality of its right-hand side to this eigenmode:

$$\frac{d\xi}{dt}\int_{-\infty}^{+\infty}\left[\frac{\partial\psi_0}{\partial\xi}\right]^2 dx\,dy=\epsilon(\gamma-\gamma_2)\int_{-\infty}^{+\infty}\psi_0\frac{\partial\psi_0}{\partial\xi}dx\,dy + \int_{-\infty}^{+\infty}G(x,y)\frac{\partial\psi_0}{\partial\xi}dx\,dy . \tag{4.31}$$

In terms of the rescaled variables

$$X\equiv\sqrt{\epsilon}x,\quad \Xi\equiv\sqrt{\epsilon}\xi,\quad T\equiv\epsilon t ,$$

and after insertion of the explicit form of ψ_0 [see Eq. (4.29)] and G, Eq. (4.31) can be written as follows:

$$\frac{d\Xi}{dT}=\left\{\int_{-\infty}^{+\infty}dX\left[\left[\frac{dA_1}{dX}\right]^2+2\left[\frac{dA_2}{dX}\right]^2\right]\right\}^{-1}\left[-(\gamma-\gamma_2)\frac{20\gamma-3-3\sqrt{1+20\gamma}}{100}+\sum_{n=1}^{4}\int_{-\infty}^{+\infty}dX\,G_n(X)\cos\frac{n(\Xi+X)}{\sqrt{\epsilon}}\right] . \tag{4.32}$$

Here

$$G_1(X)\equiv-(3A_1^2+4A_1A_2+4A_2^2)\frac{dA_1}{dX} +2A_2(A_1^2+A_2^2)\frac{dA_2}{dX} , \tag{4.33}$$

and a particular form of higher G_n is immaterial.

The crucial fact is that the integral in the last term of Eq. (4.32) is exponentially small as its integrand is a quickly oscillating function. Indeed, let us consider the analytical continuation of the function $G_1(X)$ for complex X, and designate X_s a singularity of this function nearest to the real axis (at real X this function has no singularities). Then the integral is proportional to

$$\exp[-(\mathrm{Im}X_s)/\sqrt{\epsilon}]\cos[(\Xi+\mathrm{Re}X_s)/\sqrt{\epsilon}] , \tag{4.34}$$

and Eq. (4.32) takes the form

$$\frac{d\Xi}{dT}=\frac{dc}{d\gamma}\left[(\gamma-\gamma_2)+\mathrm{const}\times\exp\left[-\frac{\mathrm{Im}X_s}{\sqrt{\epsilon}}\right]\times\cos\left[\frac{\Xi+\mathrm{Re}X_s}{\sqrt{\epsilon}}\right]\right] , \tag{4.35}$$

where $dc/d\gamma$ is taken from the amplitude equations at

$\gamma=\gamma_2$; see Eq. (4.17b). It is important that the parameter $\mathrm{Im}X_s$, although being a function of γ, is independent of the small parameter ϵ, so that the expression (4.34) is, in the general case, exponentially small in $1/\sqrt{\epsilon}$.

Thus Eq. (4.35), which is nothing but an equation of motion of the DB in the case of small $|\gamma-\gamma_2|$, coincides with the overdamped equation of motion of a particle in the sinusoidal potential relief with an exponentially small modulation depth. Evidently, the DB is trapped by the relief provided

$$|\gamma-\gamma_2|<\text{const}\times\exp\left[-\frac{\mathrm{Im}X_s}{\sqrt{\epsilon}}\right]. \tag{4.36}$$

Our final conclusion is that, on account of the nonadiabatic effects, the DB between hexagons and rolls is immobile not at the single value $\gamma=\gamma_2$, but in the exponentially narrow range (4.36).

As a matter of fact, this result can be obtained in a less formal way if one notes that the Lyapunov functional for the model (4.26) contains the "potential energy"

$$\mathcal{U}\equiv\int_{-\infty}^{+\infty}dx\,dy\,(\tfrac{1}{3}\sqrt{\epsilon}\psi^3-\tfrac{1}{12}\psi^4)\,. \tag{4.37}$$

Inserting the lowest-order approximation ψ_0 for the DB solution [see Eq. (4.29)] into Eq. (4.37), we immediately see that the interplay between the slowly varying envelope amplitudes A_l and the quickly oscillating functions $\cos(\mathbf{k}_j\cdot\mathbf{r})$ generate the same exponentially small integral which amounts to the expression (4.34). Thus the effective trapping potential directly originates from the "potential energy" (4.37) as its part amenable for the interaction of the large-scale DB with the underlying small-scale periodic pattern.

2. An explicit example

Now it is obvious that the final result (4.36) is quite general, and it can be directly applied to any model for which $\mathrm{Im}X_s$ can be found explicitly. The same estimate gives the pinning range for the DB between hexagons and the quiescent state, with the difference that ϵ must be replaced by $|\epsilon|$ and γ_2 by γ_1.

An explicit form of the DB between the hexagons and rolls is known for the case $0<g-1\ll 1$, $\theta=0$ and is given by Eqs. (4.19)–(4.23) (the second exactly tractable case, $\theta=\pi/2$, does not suit us, see below). It is easy to find that the singularity Z_s of the analytically continued solution (4.23), nearest to the real axis, has the imaginary part

$$\mathrm{Im}Z_s=\frac{\sqrt{3}-1}{4}\pi \tag{4.38}$$

[at this point, $\cos[\chi(Z_s)]=-2/\sqrt{3}$]. Taking account of the rescalings (4.5), (4.7), and (4.20), we find that Eq. (4.38) gives rise to the following estimation for the pinning range [see Eq. (4.36)]:

$$|\gamma-\gamma_2|<\text{const}\times\exp\left[-\frac{\sqrt{3}-1}{8}\pi\left[\frac{3(g-1)}{\epsilon}\right]^{1/2}\right]. \tag{4.39}$$

As is seen from the expression (4.39), the particular case $g-1\ll 1$ is, as a matter of fact, the most important one, because in this case the smallness of ϵ may be at least partially compensated by that of $(g-1)$. In the limiting case $g-1\lesssim\epsilon$, the pinning range is not exponentially small at all. Note that, according to Eqs. (4.5), (4.20), and (4.23), in this case a characteristic size (width) of the DB is comparable with the period of the underlying small-scale structure. So, a more careful analysis is required to find an accurate estimate for the pinning range in this case.

3. Absence of pinning of oblique domain boundaries

So far, we confined our attention to the case when the DB was strictly perpendicular to any of the three resonantly coupled wave vectors $\mathbf{k}_l$. To consider the general case of an oblique DB, it is convenient to employ the approach to the pinning problem based on the potential energy (4.37). If the angle θ between the wave vector and the x axis is small (recall the DB is orthogonal to the x axis), the multiplier $\cos(\mathbf{k}_l\cdot\mathbf{r})$ in Eq. (4.29) will give rise to the ones $\cos(\theta y)$ or $\sin(\theta y)$ [recall that, according to Eq. (2.2), $k_c=1$] in the integrand for the "energy" of interaction of the DB with the small-scale pattern. Taking into account the integration over y, we conclude that the full interaction energy for the oblique DB contains a small factor $\sim(\theta k_c l)^{-1}$ in comparison with the case $\theta=0$, where l is an overall length of the system in the y direction [it is implied $\theta\gtrsim(k_c l)^{-1}$]. Thus the pinning takes place at the angles $|\theta|\lesssim(k_c l)^{-1}$. Of course, we imply $k_c l\gg 1$, i.e., the overall size of the system is much greater than the internal scale $\sim k_c^{-1}$ of the periodic pattern.

D. A domain boundary near a sidewall

A sidewall creates natural conditions for appearance of the DB between hexagons and rolls. Let the wall be located at $x=0$, i.e., an amplitude of a convection pattern must vanish at $x=0$. Let us consider the case $0<\gamma<\gamma_2$ [see Eq. (4.18)], when the hexagonal pattern quenches the rolls. As is well known,[44] the sidewall always selects the roll pattern perpendicular to the wall, i.e., with the wave vector $\mathbf{k}=(0,k)$. The incompatibility of the bulk hexagonal pattern with the near-wall roll pattern is the reason for appearance of the DB.

To consider this situation in more detail, let us suppose that the orientation angles of the hexagons relative to the DB are $\theta_1=\pi/2$, $\theta_2=-\theta_3=\pi/6$. Evidently, matching this bulk pattern to the near-wall rolls can be accomplished by the DB of the roll-hexagon type located sufficiently far from the wall and parallel to it (Fig. 11). This fact was first detected in numerical simulations of the model (4.26) performed in Ref. 40. A corresponding analytical result can be obtained in the case

$$0<\gamma-\gamma_2\ll\gamma_2\,, \tag{4.40}$$

when the rolls are close to equilibrium with the hexagons. To do this, let us note that the system can be formally extended to the unphysical region $x<0$ as follows:

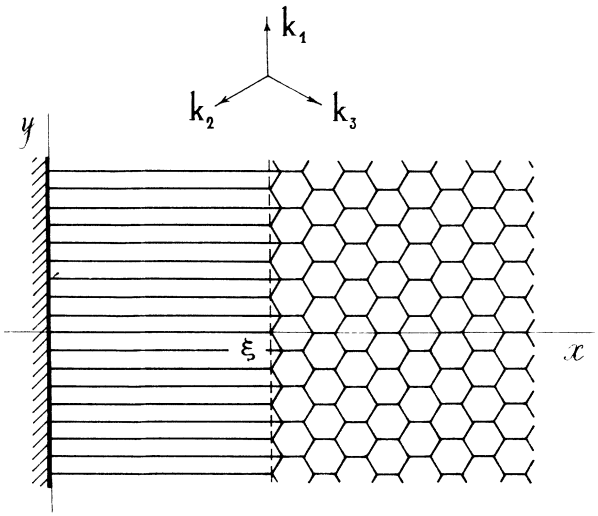

FIG. 11. The domain boundary (depicted by the vertical dashed line) matching the bulk hexagonal pattern to the near-sidewall rolls.

$$A_l(-x)=-A_l(x), \quad l=2,3 \tag{4.41}$$

which guarantees that the boundary conditions $A_l(0)=0$ are satisfied.[46] If the system contains the DB roll-hexagon at a large distance ξ from the wall, Eqs. (4.41) imply that another DB (its mirror image) is located at $x=-\xi$. One can analyze interaction of the two DB's following the lines of the approach developed in Ref. 45. They repel each other (an effective interaction potential is exponential), while the "pressure" of the bulk hexagonal pattern tends to press them to each other. The effective equation of motion for the system of two DB's takes the form

$$\frac{d\xi}{dt}=\frac{dc}{d\gamma}(\gamma-\gamma_2)+\text{const}\times\exp(-2\lambda_2\xi) , \tag{4.42}$$

where $dc/d\gamma$ is taken as for a solitary DB [see Eq. (4.17b)], and the constant λ_2 is a minimum spatial rate of damping of disturbances on the background of the roll pattern. The linearized equations (4.6), together with Eqs. (4.5) and (4.7), yield

$$\lambda_2=\{[(g-1)\gamma_2-\sqrt{\gamma_2}]\epsilon/3\gamma_2\}^{1/2} , \tag{4.43}$$

where γ_2 is given by Eq. (4.18). In particular, in the limiting case $g-1\ll 1$ the exponent λ_2 becomes anomalously small $\sim(g-1)^{1/2}$ according to Eqs. (4.43) and (4.18).

As follows from Eq. (4.42), in the stable stationary state the DB takes the equilibrium position

$$\xi_0\approx\frac{1}{2\lambda_2}\ln(\gamma_2-\gamma)^{-1} . \tag{4.44}$$

Evidently, at $\gamma>\gamma_2$ the DB detaches from the sidewall and quenches the hexagons in the bulk of the system.

An analogous situation takes place at $\gamma_1<\gamma<0$ [see Eq. (4.16)], when the subcritical hexagonal pattern quenches the quiescent state which is, however, sustained by the boundary conditions at the wall ($x=0$). As a result, we obtain the DB of the quiescent-state–hexagon type parallel to the wall. Note that the orientation of the hexagons relative to the DB may be arbitrary in this case. The equation of motion for the DB and the expression for its equilibrium position ξ_0 take the form of Eqs. (4.42) and (4.44) with γ_2 substituted by γ_1 and λ_2 substituted by another constant λ_1, which, as well as λ_2 [see Eq. (4.43)], is $\sim|\epsilon|^{1/2}$. An explicit formula for λ_1 can be obtained, but it is rather cumbersome.

E. Resonant domain boundary "roll-roll"

Let us consider DB between two systems of rolls in the case when $\gamma>\gamma_2$, and the angle between their wave vectors is equal to $\pi/3$ or $2\pi/3$. In the region of their overlapping, the resonant interaction will give rise to a third system that constitutes a resonance triad with the original ones. Thus we will have a layer of hexagons sandwiched between the rolls. If the parameter $(\gamma-\gamma_2)$, proportional to the pressure exerted by the bulk roll patterns upon the hexagonal layer, is sufficiently small, the DB may be regarded as a bound state of two DB's of the type roll-hexagon which repel each other; cf. the situation considered in the preceding section. The effective potential of the repulsion is again exponential $\sim\exp(-\lambda\xi)$, where ξ is distance between the two DB's, and λ is a minimum spatial rate of damping of disturbances on the background of the hexagonal pattern. If the DB is oblique, an expression for λ in terms of ϵ, α, and orientation angles is very cumbersome. This expression takes on a simple form in the case $g-1\ll 1$ in two symmetric configurations shown in Fig. 12: If any wave vector $\mathbf{k}_l$ is perpendicular to the DB ($\theta_l=0$),

$$\lambda=\tfrac{1}{3}[(g-1)\epsilon]^{1/2} ,$$

and if $\mathbf{k}_l$ is parallel to the DB ($\theta_l=\pi/2$),

$$\lambda=[\tfrac{1}{3}(g-1)\epsilon]^{1/2} ,$$

cf. Eq. (4.43). Finally, at small $(\gamma-\gamma_2)$, the equilibrium distance between the DB's is [cf. Eq. (4.44)]

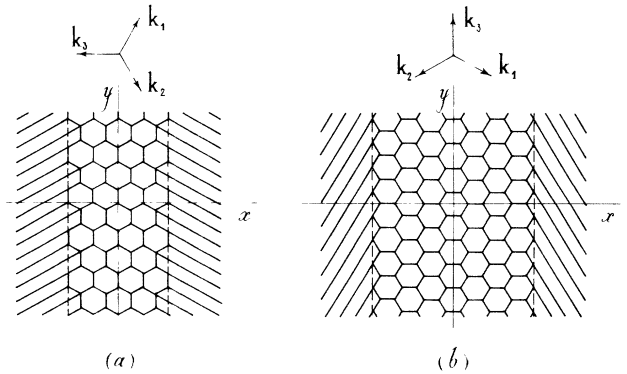

FIG. 12. The resonant domain boundary between the rolls: (a) $\theta_3=0$; (b) $\theta_3=\pi/2$.

$$\xi_0 \approx \lambda^{-1} \ln(\gamma - \gamma_2)^{-1} .$$

At $\gamma < \gamma_2$ the intermediate hexagonal phase quenches the roll pattern.

V. DOMAIN BOUNDARY BETWEEN RECTANGULAR PATTERNS

As was mentioned above, the roll pattern is unstable in the case when there is an angle θ such that the nonlinear coupling parameter $g(\theta) \equiv \kappa(\theta)/\kappa(0)$ lies in the range $g(\theta) < 1$. In this case a rectangular pattern[21] (its particular form is a square pattern[19,20]) sets in. This pattern is given by Eq. (2.4) with $N=2$. Stability conditions for the rectangular patterns have been studied in detail in Ref. 21. Here we will consider DB between rectangles with different orientations. The simplest case is that shown in Fig. 13, when the wave vector $\mathbf{k}_0$ is common for both patterns, $\mathbf{k}_0$ being parallel to the DB, and $|\mathbf{k}_0| = |\mathbf{k}_1| = |\mathbf{k}_2| = 1$. Thus we deal with three amplitudes a_0, a_1, and a_2. After the usual rescaling (3.3b), the coupled Ginzburg-Landau equations for them take the form [cf. Eqs. (3.8)]

$$(A_0)_T = (1 - |A_0|^2 - g_1 |A_1|^2 - g_2 |A_2|^2) A_0 , \tag{5.1a}$$

$$(A_1)_T = D_1 (A_1)_{XX} + (1 - |A_1|^2 - g_1 |A_0|^2 - g_{12} |A_2|^2) A_1 , \tag{5.1b}$$

$$(A_2)_T = D_2 (A_2)_{XX} + (1 - |A_2|^2 - g_2 |A_0|^2 - g_{12} |A_1|^2) A_2 , \tag{5.1c}$$

where $g_1 \equiv g(\theta_1)$, $g_2 \equiv g(\theta_2)$, $g_{12} \equiv g(\theta_1 + \theta_2)$, and, according to Eq. (3.10), $D_l \equiv \cos^2 \theta_l$ ($l = 1,2$). In Eq. (5.1a), where $D_0 = 0$, we have neglected the fourth derivative [see Eqs. (2.5)]. The boundary conditions specifying the DB solution are obvious:

$$A_2 = 0, \quad A_0 = A_1 \equiv A(\theta_1) \quad \text{at } X = -\infty , \tag{5.2a}$$

$$A_1 = 0, \quad A_0 = A_2 \equiv A(\theta_2) \quad \text{at } X = +\infty , \tag{5.2b}$$

where $A(\theta_l) \equiv [1 + g(\theta_1)]^{-1/2}$. In what follows, we will confine ourselves to the symmetric case $\theta_1 = \theta_2 \equiv \theta$, and we will assume the amplitudes real and time independent. In this case Eq. (5.1a) yields

$$A_0^2 = 1 - g(A_1^2 + A_2^2)$$

and Eqs. (5.1b) and (5.1c) take the form

$$\frac{D}{1-g^2}(A_1)_{XX} + \frac{1}{1+g} A_1 - A_1^3 - \frac{g_{12} - g^2}{1-g^2} A_2^2 A_1 = 0 , \tag{5.3a}$$

$$\frac{D}{1-g^2}(A_2)_{XX} + \frac{1}{1+g} A_2 - A_2^3 - \frac{g_{12} - g^2}{1-g^2} A_1^2 A_2 = 0 , \tag{5.3b}$$

where $g(\theta_1) = g(\theta_2) \equiv g$, $D_1 = D_2 \equiv D$. As a matter of fact, Eqs. (5.3) coincide with the stationary version of Eqs. (3.8), and the results obtained in Sec. II can be applied to the present problem. In particular, an exact solution analogous to that of (3.26) can be found at $g_{12} = 3 - 2g^2$.

VI. CONCLUSION

The appearance of, generally speaking, moving DB's (fronts) between hexagons and rolls (at $\epsilon > 0$) or the quiescent state (at $\epsilon < 0$) is an inevitable consequence of hysteretic coexistence of these patterns. Besides, we have demonstrated that the immobile DB between rolls and hexagons is necessary to accord the hexagonal pattern (in the case when it quenches the rolls) with the boundary conditions at the lateral wall. The same pertains to the DB between hexagons and the quiescent state in the case when the hexagons dominate.

Possibilities for experimental implementation of the DB between rolls with different orientations are less clear.[47] Nevertheless, linear defects resembling DB's of this type can be seen in experimental patterns reported, e.g., in Refs. 8 and 48–50. It seems to us that DB's of different types deserve further experimental investigation.

In conclusion, we would like to mention some unresolved theoretical problems which seem physically interesting. One of them is a "triple point," at which three halves of DB's of the roll-roll type meet (Fig. 14). It remains unknown under which conditions this configuration is in equilibrium, and how it will move in a nonequilibrium case. Note that this configuration must

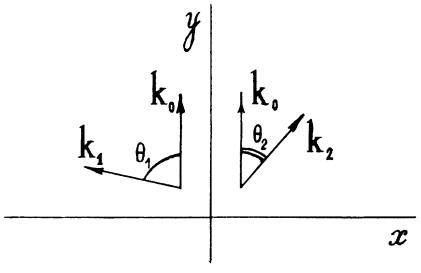

FIG. 13. The wave vectors of two rectangular patterns matched via the domain boundary parallel to the y axis. The wave vector $\mathbf{k}_0$ is common for both patterns.

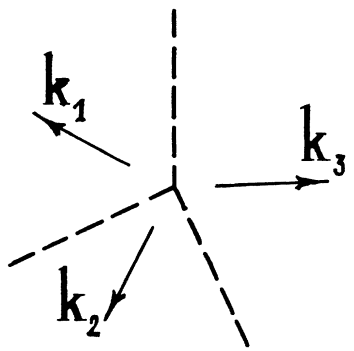

FIG. 14. The "triple-point" configuration in a roll pattern.

occur as a generic one in a large-size system with a disordered initial state (it can be implemented experimentally if the sidewalls possess the "heat transparency"[51]). Another interesting problem is evolution of a curved DB. This problem seems especially intriguing for a DB involving the hexagonal pattern because, as was demonstrated in the present paper, the velocity of such a DB is anisotropic (although the anisotropy is, in fact, weak).

---

*Permanent address: Department of Mathematics, Technion, Haifa 32000, Israel.

[1]G. L. Gershuni and E. M. Zhukhovitsky, *Convective Stability of an Incompressible Liquid* (Nauka, Moscow, 1972) (in Russian) [English translation: (Keter, Jerusalem, 1976)].

[2]F. H. Busse, Rep. Prog. Phys. **41**, 1930 (1978).

[3]F. H. Busse and J. A. Whitehead, J. Fluid Mech. **47**, 305 (1971).

[4]V. Croquette and A. Pocheau, in *Cellular Structures in Instabilities*, Vol. 210 of *Lecture Notes in Physics*, edited by J. E. Wesfreid and S. Zaleski (Springer-Verlag, Berlin, 1984), p. 104.

[5]J. P. Gollub, in Ref. 4, p. 156.

[6]E. D. Siggia and A. Zippelius, Phys. Rev. A **15**, 319 (1981).

[7]Y. Pomeau, P. Manneville, and S. Zaleski, Phys. Rev. A **27**, 2710 (1983).

[8]A. Pocheau and V. Croquette, J. Phys. (Paris) **45**, 35 (1984).

[9]G. Tesauro and M. C. Cross, Phys. Rev. A **34**, 1363 (1986).

[10]Y. Shiwa and K. Kawasaki, J. Phys. A **19**, 1387 (1986).

[11]M. C. Cross, Phys. Rev. A **25**, 1065 (1982).

[12]P. Manneville and Y. Pomeau, Philos. Mag. A **48**, 607 (1983).

[13]M. C. Cross, G. Tesauro, and H. S. Greenside, Physica D **23**, 12 (1986).

[14]Y. Pomeau, Physica D **23**, 3 (1986).

[15]A. C. Newell and J. A. Whitehead, J. Fluid Mech. **38**, 279 (1969).

[16]L. A. Segel, J. Fluid Mech. **38**, 203 (1969).

[17]L. A. Segel, J. Fluid Mech. **21**, 359 (1965).

[18]F. H. Busse, J. Fluid Mech. **30**, 625 (1967).

[19]F. H. Busse and N. Riahi, J. Fluid Mech. **96**, 243 (1980).

[20]V. L. Gertsberg and G. I. Sivashinsky, Prog. Theor. Phys. **66**, 1219 (1982).

[21]B. A. Malomed and M. I. Tribelsky, Zh. Eksp. Teor. Fiz. **92**, 539 (1987) [Sov. Phys.—JETP **65**, 305 (1987)].

[22]B. A. Malomed, A. A. Nepomnyashchy, and M. I. Tribelsky, in *Nonlinear World*, edited by A. G. Sitenko, V. E. Zakharov, and V. M. Chernousenko (Naukova Dumka, Kiev, 1989), Vol. 1, p. 143.

[23]R. Ribbota and A. Joets, in Ref. 4, p. 249.

[24]L. Kramer *et al.*, Liq. Cryst. **5**, 699 (1989).

[25]A. Schlüter, D. Lortz, and F. Busse, J. Fluid Mech. **23**, 129 (1965).

[26]V. S. Sorokin, Prikl. Mat. Mekh. **18**, 187 (1954) [in Russian].

[27]B. A. Malomed and M. I. Tribelsky, Prikl. Mat. Mekh. **52**, 70 (1988) [PMM (USSR) **52**, 53 (1988)].

[28]B. A. Malomed, A. A. Nepomnyashchy, and M. I. Tribelsky, Pis'ma Zh. Tekh. Fiz. **13**, 1165 (1987) [Sov. Tech. Phys. Lett. **13**, 487 (1987)]; Zh. Eksp. Teor. Fiz. **96**, 688 (1989) [Sov. Phys.—JETP **69**, 388 (1989)].

[29]G. Dee and J. S. Langer, Phys. Rev. Lett. **50**, 383 (1983); G. Dee, Physica D **15**, 295 (1985).

[30]A. A. Nepomnyashchy (unpublished).

[31]Note that the underlying equations (3.1) have been written without the "natural" multiplier 2 in front of $\kappa(\theta_1-\theta_2)$, see Ref. 28, so that $\lim_{\theta\to 0} g(\theta)=2g(0)$, where $\theta\equiv\theta_1-\theta_2$.

[32]M. C. Cross, P. G. Daniels, P. C. Hohenberg, and E. D. Siggia, J. Fluid Mech. **127**, 155 (1983).

[33]L. Kramer, E. Ben-Jacob, H. Brand, and M. C. Cross, Phys. Rev. Lett. **49**, 1891 (1981).

[34]Yu. G. Vasilenko *et al.*, Zh. Prikl. Mekh. Tekn. Fiz. **2**, 58 (1980).

[35]B. A. Malomed, Physica D **8**, 353 (1983).

[36]M. C. Cross and A. C. Newell, Physica D **10**, 299 (1984).

[37]Y. Pomeau and P. Manneville, J. Phys. Lett. (Paris) **40**, 609 (1979).

[38]J. W. Cahn, Acta Metall. **14**, 1685 (1966).

[39]A. Novick-Cohen and L. A. Segel, Physica D **10**, 277 (1984).

[40]M. Bestehorn and H. Haken, Phys. Lett. **99A**, 265 (1983).

[41]J. S. Langer, Rev. Mod. Phys. **52**, 1 (1980).

[42]D. Bensimon, B. I. Shraiman, and V. Croquette, Phys. Rev. A **38**, 5461 (1988).

[43]J. Swift and P. C. Hohenberg, Phys. Rev. A **15**, 319 (1977).

[44]S. Zaleski, Y. Pomeau, and A. Pumir, Phys. Rev. A **29**, 366 (1984).

[45]K. Kawasaki and T. Ohta, Physica A **116**, 573 (1982).

[46]In Eq. (4.41) $l\neq 1$ since in the case considered $(\theta_1=\pi/2)D_1=0$, hence Eq. (4.6) for A_1 is not a differential one and a boundary condition for $A_1(X)$ is not needed. However, it is easy to see that the amplitude A_1 defined by Eqs. (4.6) and (4.41) does not satisfy the physical boundary condition $A_1(0)=0$ [see, for instance, the expression (2.49) with $\chi=0$]. The contradiction is lifted if we take into account the higher derivatives omitted in Eq. (4.6) [see, e.g., Eqs. (3.72) and (3.73)]. They provide existence of a narrow layer in a vicinity of the sidewall where $A_1(X)$ vanishes.

[47]However, they must appear in a large-aspect-ratio convection cell of a polygonal form, in order to adjust the roll pattern to sidewalls.

[48]G. Ahlers, D. S. Cannell, and V. Steinberg, Phys. Rev. Lett. **54**, 1373 (1985).

[49]V. Steinberg, G. Ahlers, and D. S. Cannell, Phys. Scr. **32**, 534 (1985).

[50]M. S. Heutmaker, P. N. Fraenkel, and J. P. Gollub, Phys. Rev. Lett. **54**, 1369 (1985).

[51]G. Ahlers, C. W. Meyer, and D. S. Cannell, J. Stat. Phys. **54**, 1121 (1989).